molecules

MDPI

Article

Crystal Structures of Xenon(VI) Salts: $XeF_5Ni(AsF_6)_3$, XeF_5AF_6 (A = Nb, Ta, Ru, Rh, Ir, Pt, Au), and $XeF_5A_2F_{11}$ (A = Nb, Ta)

Zoran Mazej * and Evgeny Goreshnik

Department of Inorganic Chemistry and Technology, Jožef Stefan Institute, Jamova Cesta 39, SI-1000 Ljubljana, Slovenia; evgeny.goreshnik@ijs.si

* Correspondence: zoran.mazej@ijs.si

Abstract: Experiments on the preparation of the new mixed cations $XeF_5M(AF_6)_3$ (M = Cu, Ni; A = Cr, Nb, Ta, Ru, Rh, Re, Os, Ir, Pt, Au, As), $XeF_5M(SbF_6)_3$ (M = Sn, Pb), and $XeF_5M(BF_4)_x(SbF_6)_{3-x}$ (x = 1, 2, 3; M = Co, Mn, Ni, Zn) salts were successful only in the preparation of $XeF_5Ni(AsF_6)_3$. In other cases, mixtures of different products, mostly XeF_5AF_6 and $XeF_5A_2F_{11}$ salts, were obtained. The crystal structures of $XeF_5Ni(AsF_6)_3$, XeF_5TaF_6, XeF_5RhF_6, XeF_5IrF_6, $XeF_5Nb_2F_{11}$, $XeF_5Ta_2F_{11}$, and $[Ni(XeF_2)_2](IrF_6)_2$ were determined for the first time on single crystals at 150 K by X-ray diffraction. The crystal structures of XeF_5NbF_6, XeF_5PtF_6, XeF_5RuF_6, XeF_5AuF_6, and $(Xe_2F_{11})_2(NiF_6)$ were redetermined by the same method at 150 K. The crystal structure of XeF_5RhF_6 represents a new structural type in the family of XeF_5AF_6 salts, which crystallize in four different structural types. The $XeF_5A_2F_{11}$ salts (M = Nb, Ta) are not isotypic and both represent a new structure type. They consist of $[XeF_5]^+$ cations and dimeric $[A_2F_{11}]^-$ anions. The crystal structure of $[Ni(XeF_2)_2](IrF_6)_2$ is a first example of a coordination compound in which XeF_2 is coordinated to the Ni^{2+} cation.

Keywords: metal; fluorine; xenon; crystal structure; Raman spectroscopy; photochemistry

Citation: Mazej, Z.; Goreshnik, E. Crystal Structures of Xenon(VI) Salts: $XeF_5Ni(AsF_6)_3$, XeF_5AF_6 (A = Nb, Ta, Ru, Rh, Ir, Pt, Au), and $XeF_5A_2F_{11}$ (A = Nb, Ta). *Molecules* **2023**, *28*, 3370. https://doi.org/10.3390/molecules28083370

Academic Editors: Sergey A. Adonin and Artem L. Gushchin

Received: 20 March 2023
Revised: 7 April 2023
Accepted: 9 April 2023
Published: 11 April 2023

1. Introduction

The synthesis of XeF_6 was first described in 1962 [1]. It was prepared by the reaction between xenon and fluorine (molar ratio 1:20) at 700 °C and a pressure of ~200 bar F_2. Later systematic studies showed that XeF_6 can be prepared under milder conditions (molar ratio 1:10; 200 °C; and a total pressure of 33 bar) [2]. In general, XeF_6 is prepared by heating a mixture of Xe and F_2 (molar ratio 1:20) at 300 °C and a total pressure of ~50 bar [3]. In the presence of a NiF_2 catalyst, XeF_6 forms explosively from the gaseous mixture of xenon and fluorine in a molar ratio of 1:5 already at 120 °C [4]. An alternative method with high yield for the preparation of high-purity XeF_6 is the reaction between Xe and F_2 at low pressure and high filament temperature in a "hot wire" reactor [5]. At room temperature, XeF_6 is solid ($T_{m.p.}$ = 49.48 °C, $T_{b.p.}$ = 75.57 °C) with a vapor pressure of about 0.03 bar at 23 °C [6]. The color of solid XeF_6 has been reported to range from colorless to intense yellow. An explanation for these color variations of solid XeF_6 is not apparent to date [7]. Liquid XeF_6 and its vapors are yellow-green [6]. There are six, possibly seven, different modifications of solid XeF_6 [7]. In CF_2Cl_2/SO_2ClF solution, XeF_6 exists as a tetramer $(XeF_6)_4$ [8], while in the gas phase XeF_6 exists as a monomer [9–11]. The presence of a sterically active free valence electron pair on Xe leads to the XeF_6 molecule being fluxional [12]. Consequently, the structure of monomeric XeF_6 has been a major challenge for theoretical computational chemistry [12–17]. Experiments have clearly shown that XeF_6 is not octahedral (O_h) but most likely has the shape of a slightly distorted octahedron (C_{3v}), naturally in a dynamical form [18]. Both conformers are energetically very close to each other [15]. Because of the low barrier of interconversion, XeF_6 is a highly fluoxinal molecule that rapidly converts between the 8-fold degenerate C_{3v} structures via the octahedral minimum even at low temperatures [15]. In further studies, XeF_6 was theoretically shown to exhibit a genuine quantum mechanical fluorine tunneling rearrangement, where it "jumps"

rapidly between isomers even near 0 K [16]. In solid argon and neon matrices, there are significant interactions between isolated XeF_6 monomers and the noble gas host [15]. The results of infrared spectroscopy of XeF_6 in Ne matrix, supported by theoretical calculations, agreed with the C_{3v} conformer [15].

Shortly after the first report on the synthesis of XeF_6, it was found that XeF_6 is a good fluoride ion donor that reacts with Lewis acids AF_5 (A = As, Sb, Pt, V, P) to form $nXeF_6 \cdot AF_5$ adducts [19–23]. Crystal structure determination of $XeF_6 \cdot PtF_5$ revealed a molecular geometry consistent with the ionic formula $[XeF_5]^+[PtF_6]^-$ [24]. The compounds $XeF_6 \cdot 2AF_5$ are also $[XeF_5]^+$ salts [25], while the compounds $2XeF_6 \cdot AF_5$ are $[Xe_2F_{11}]^+$ salts [26–28]. The next step was the discovery that XeF_5AF_6 salts can bind neutral molecules as XeF_2 [29–31]. Later, this was extended to HF [32], $XeOF_4$ [33], and even KrF_2 [32]. Recently, the XeF_5SbF_6 salt was also found to react with other $MSbF_6$ and $M(SbF_6)_2$ salts to give $XeF_5M(SbF_6)_2$ (M = NO_2^+, Rb^+, Cs^+) [28,34], $XeF_5M(SbF_6)_3$ (M^{2+} = Mg, Mn, Co, Ni, Cu, Zn, Pd), and $(XeF_5)_3[M(HF)_2](SbF_6)_7$ (M = Hg) [34,35] or even more complex salts $(H_3O)(XeF_5)_2M_2(SbF_6)_7 \cdot nHF$ (M = Ca, Cd) [36] and $(O_2)(XeF_5)_2Sr_4(SbF_6)_{11} \cdot 8HF$ [36] with three different cations. In addition, mixed anion salts $Cs[XeF_5][Bi_xSb_{1-x}F_6]$ [28] and $[XeF_5][As_{1-x}Sb_xF_6)$ (x~0.5 and 0.7) [37] have also been reported.

XeF_6 is a stronger oxidizing and fluorinating agent than XeF_2 and XeF_4. Theoretically, XeF_6 could be used as a fluorinating agent. Unfortunately, XeF_6 and its XeF_5^+ salts are very sensitive to moisture. When they are exposed to water, they hydrolyze and eventually form XeO_3. The latter is an unstable compound that is extremely sensitive to impact and poses a dangerous explosion hazard when in contact with organic materials. For this reason, XeF_6 and its XeF_5^+ salts currently have no practical significance.

This contribution reports the results of experiments on the preparation of $XeF_5M(SbF_6)_3$ (M = Sn, Pb), $XeF_5M(BF_4)_x(SbF_6)_{3-x}$ (x = 1, 2, 3; M = Co, Mn, Ni, Zn), and $XeF_5M(AF_6)_3$ salts (M = Cu, Ni; A = Cr, Nb, Ta, Ru, Rh, Re, Os, Ir, Pt, Au, As). The experiments were successful only in the preparation of $XeF_5Ni(AsF_6)_3$, and many other phases were obtained in other experiments. The crystal structures of $XeF_5Nb_2F_{11}$, XeF_5TaF_6, $XeF_5Ta_2F_{11}$, XeF_5RhF_6, XeF_5IrF_6, and $Ni(XeF_2)_2(IrF_6)_2$ were determined for the first time. The crystal structures of XeF_5NbF_6 [30], XeF_5PtF_6 [24], XeF_5RuF_6 [38], XeF_5AuF_6 [39], and $(Xe_2F_{11})_2(NiF_6)$ [40] were redetermined with higher accuracy than previously reported.

2. Results

2.1. Attempted Preparation of the Salts $XeF_5M(AF_6)_3$ (M = Cu, Ni; A = Cr, Nb, Ta, Ru, Rh, Re, Os, Ir, Pt, Au, As), $XeF_5M(SbF_6)_3$ (M = Sn, Pb), and $XeF_5M(BF_4)_x(SbF_6)_{3-x}$ (x = 1, 2, 3; M = Co, Mn, Ni, Zn)

The proposed synthetic methods lead to a mixture of substances. The work carried out is an X-ray diffraction study of some crystal phases of these mixtures. In addition, some of the products were also confirmed by Raman spectroscopy (Supplementary Materials).

Reactions between XeF_2, MF_2 (M = Cu, Ni), AsF_5, and UV-irradiated F_2 in anhydrous hydrogen fluoride (aHF) resulted in clear colorless (Cu) and yellow (Ni) solutions (Table S1). In the case of nickel, single crystals of $XeF_5Ni(AsF_6)_3$ were obtained upon crystallization (Table 1), while in the case of copper a mixture of single crystals of XeF_5AsF_6 [41] and $CuFAsF_6$ [42] was observed in the crystallization product. In all other experiments where mixtures of XeF_2/MF_2 (M = Ni, Cu) with addition of AF_3 (A = Cr, Au), AF_5 (A = Nb, Ta), or metal powder A (A = Re, Ru, Rh, Os, Ir, Pt) were treated with UV-irradiated F_2 (Table S1), the insoluble material did not disappear even after several days. For crystallization, the clear supernatant, which contained no visible sediments, was decanted into the side arm of the double-arm crystallization vessel. Only single crystals of XeF_5AF_6 (A = Nb, Ta, Ru, Rh, Ir, Pt, Au) and $XeF_5A_2F_{11}$ salts (A = Nb, Ta) were grown from the corresponding solutions (Table S1). In the case of Ru and Pt, traces of O_2AF_6 salts (A = Ru, Pt) [43,44] were also present. Although the remaining insoluble solids were not characterized, it can be assumed that they probably consisted of $M(AF_6)_2$ salts (M = Ni, Cu; A = Nb, Ta, Ru, Rh, Ir, Pt, Au). Of these, only $Cu(AuF_6)_2$ and $Ni(AuF_6)_2$ [45] are known, while the others have not yet been synthesized. Similar to the $M[AuF_6]_2$ salts, unlike the $M(AF_6)_2$ salts (A = As, Sb) [46],

they are probably not well soluble or they are insoluble in anhydrous HF. For the $M(AF_6)_2$ salts (M = Ni, Cu; A = Nb, Ta, Ru, Rh, Os, Ir, Pt), their lattice energy appears to overcome the solvation energy. This would explain their insolubility in aHF and the preferential formation of mixtures of $M(AF_6)_2$ (insoluble in aHF) and XeF_5AF_6 (soluble in aHF) instead of $XeF_5M(AF_6)_3$ salts (M = Cu, Ni; A = Nb, Ta, Ru, Rh, Ir, Pt, Au).

Table 1. Summary of crystal data and refinement results for XeF_5AF_6 (A = Nb, Ta, Ru, Rh, Ir, Pt, Au).

Formula	**XeF_5NbF_6**	**XeF_5TaF_6**	**XeF_5RuF_6**	**XeF_5RhF_6**
***T* (K)**	**150**	**150**	**150**	**150**
Crystal System	**Orthorhombic**	**Orthorhombic**	**Orthorhombic**	**Orthorhombic**
Space Group	***Pnma***	***Pnma***	***Pnma***	***Pbca***
a (Å)	16.8078 (10)	16.8312 (12)	16.6197 (12)	9.0028 (4)
b (Å)	8.2491 (6)	8.2399 (6)	8.0530 (6)	8.8181 (4)
c (Å)	5.6064 (3)	5.6488 (4)	5.6373 (4)	18.2581 (8)
V (Å^3)	777.32 (8)	783.41 (10)	754.49 (9)	1449.47 (11)
Z	4	4	4	8
D_{calcd} (g/cm^3)	3.702	4.419	3.886	4.062
λ (Å)	0.71073	0.71073	0.71073	0.71073
μ (mm^{-1})	5.988	18.436	6.652	7.118
GOF [a]	1.091	1.052	1.109	1.044
R_1 [b]	0.0253	0.0355	0.0244	0.0226
wR_2 [c]	0.0503	0.0757	0.0521	0.0430
Formula	**XeF_5IrF_6**	**XeF_5IrF_6**	**XeF_5PtF_6**	**XeF_5AuF_6**
***T* (K)**	**150**	**285**	**150**	**150**
Crystal System	**Orthorhombic**	**Orthorhombic**	**Orthorhombic**	**Monoclinic**
Space Group	***Pnma***	***Pnma***	***Pnma***	***$P2_1/c$***
a (Å)	16.5720 (10)	16.7456 (14)	16.5286 (13)	5.8447 (5)
b (Å)	7.9954 (5)	8.1444 (8)	7.9642 (5)	16.6324 (10)
c (Å)	5.7412 (4)	5.6998 (6)	5.7779 (5)	8.0536 (5)
β (^{o})				90.781 (6)
V (Å^3)	760.71 (8)	777.35 (13)	760.58 (10)	782.82 (9)
Z	4	4	4	4
D_{calcd} (g/cm^3)	4.650	4.550	4.675	4.559
λ (Å)	0.71073	0.71073	0.71073	0.71073
μ (mm^{-1})	22.088	21.615	22.986	23.202
GOF [a]	1.081	1.174	1.078	1.064
R_1 [b]	0.0267	0.0398	0.0247	0.0364
wR_2 [c]	0.0491	0.0815	0.0445	0.0798

[a] GOF = $[\Sigma w(F_o^2 - F_c^2)^2/(N_o - N_p)]^{1/2}$, where N_o = no. of reflns and N_p = no. of refined parameters. [b] $R_1 = \Sigma||F_o| - |F_c||/\Sigma|F_o|$. [c] $wR_2 = [\Sigma w(F_o^2 - F_c^2)^2/\Sigma(w(F_o^2)^2]^{1/2}$.

In the $XeF_2/NiF_2/Ir$/UV-irradiated F_2/aHF system single crystals of XeF_5IrF_6 and $Ni(XeF_2)_2(IrF_6)_2$ were found in the same batch after crystallization (Table S1). This means that either the F_2 concentration was too low to oxidize all of the Xe(II) to Xe(VI), or that partial reduction of Xe(VI) occurred during crystallization.

In the $XeF_2/NiF_2/Re$/UV-irradiated F_2 system, few single crystals of $(Xe_2F_{11})_2(NiF_6)$ were detected as crystallization product (Table S1). When pure Re powder is treated with UV-irradiated F_2 in aHF, it oxidizes to volatile ReF_6 [47]. The latter does not react in aHF even with a very good fluorine ion donor such as CsF [47]. In the $XeF_2/NiF_2/Re$/UV-irradiated F_2/aHF system, all the Re is oxidized to inert gaseous ReF_6. When the NiF_2/F_2 reaction mixture in aHF is irradiated with UV light, the particles of pale yellow-green NiF_2, which is insoluble in aHF, turn black. This indicates that NiF_2 is first fluorinated to NiF_{2+x} ($x \leq 1$) [47]. When only XeF_2 (Xe^{II}) is present without other compounds, XeF_2 is oxidized to Xe^{IV} (XeF_4) by elemental fluorine under UV light in aHF [47]. Our experiment has shown

that in the presence of Ni(II) and Xe(II) as reagents, oxidation to Ni(IV) and Xe(VI) occurs, giving $(Xe_2F_{11})_2(NiF_6)$ [40]. The A'_2NiF_6 salts (A' = Li, Na, K, Cs) can also be prepared by oxidation of NiF_2 at about 20 °C by sunlight or UV-irradiated F_2 in liquid aHF containing dissolved alkali metal fluorides (LiF, NaF, KF, CsF) [48].

In the $XeF_2/CuF_2/Os$/UV-irradiated F_2/HF system, a colorless solution was observed over white insoluble material. Upon cooling the reaction vessel to 77 K, a strong yellow coloration of the solid aHF was observed, indicating the presence of yellow OsF_6 [49]. When crystallized from the decanted clear solution, only two small colorless crystals were formed. One of them was detected as XeF_4 by Raman spectroscopy, while the other exploded on the diffractometer goniometer.

An attempt to prepare $XeF_5Cu(CrF_6)_3$ or to detect the formation of XeF_5CrF_6 salt was unsuccessful. Crystallization yielded only single crystals of $(XeF_5CrF_5)_4 \cdot XeF_4$ [50]. Although $A'CrF_6$ salts (A' = Na, K, Rb, Cs) are known [51], the salt $XeF_5^+CrF_6^-$ is not. The reaction between CrF_5 and XeF_6 proceeds at room temperature in aHF with release of fluorine and formation of XeF_5CrF_5 [52]. In the presence of XeF_4, the very stable $(XeF_5CrF_5)_4 \cdot XeF_4$ is formed [50].

Attempts to prepare $XeF_5M(SbF_6)_3$ salts (M = Sn, Pb) failed (Table S1). The crystals grown from clear decanted solutions corresponded mainly to $XeF_5Sb_2F_{11}$ [25] and XeF_5SbF_6 [25]. Various approaches to prepare $XeF_5M(BF_4)_x(SbF_6)_{3-x}$ salts (x = 1, 2, 3; M = Co, Mn, Ni, Zn) also failed. In the case of Co and Mn, oxidation of M(II) to M(III) occurred, while only crystals of XeF_5SbF_6 and $XeF_5Sb_2F_{11}$ were found between powdered material. In an attempt to prepare $(XeF_5)Ni(BF_4)_3$, only single crystals of XeF_5BF_4 [28] were found (Table S1).

2.2. Crystal Structures of the Salts XeF_5AF_6 (A = Nb, Ta, Ru, Rh, Ir, Pt, Au), $XeF_5A_2F_{11}$ (A = Nb, Ta), $(Xe_2F_{11})_2(NiF_6)_2$, and $Ni(XeF_2)_2(IrF_6)_2$

Crystal structures were determined on single crystals by X-ray diffraction. Details of the data acquisition parameters and other crystallographic information for the salts XeF_5AF_6 (A = Nb, Ta, Ru, Rh, Ir, Pt, Au), $XeF_5A_2F_{11}$ (A = Nb, Ta), and $(Xe_2F_{11})_2(NiF_6)_2$ and $Ni(XeF_2)_2(IrF_6)_2$ are given in Tables 1 and 2. The crystal structures of XeF_5NbF_6 [30], XeF_5PtF_6 [24], XeF_5RuF_6 [38], XeF_5AuF_6 [39], and $(Xe_2F_{11})_2(NiF_6)$ [40] were redetermined at low temperature with higher accuracy than previously reported.

Table 2. Summary of crystal data and refinement results for $XeF_5A_2F_{11}$ (A = Nb, Ta), $XeF_5Ni(AsF_6)_3$, $(Xe_2F_{11})_2(NiF_6)_2$, and $Ni(XeF_2)_2(IrF_6)_2$.

Formula	$XeF_5Nb_2F_{11}$	$XeF_5Ta_2F_{11}$	$XeF_5Ni(AsF_6)_3$	$(Xe_2F_{11})_2(NiF_6)_2$	$Ni(XeF_2)_2(IrF_6)_2$
***T* (K)**	**150**	**150**	**150**	**150**	**150**
Crystal System	**Monoclinic**	**Monoclinic**	**Monoclinic**	**Monoclinic**	**Monoclinic**
Space Group	***P2₁***	***I2/a***	***P2₁/n***	***I2/c***	***P2₁/c***
a (Å)	5.2717 (2)	8.9972 (5)	10.2200 (3)	17.2498 (11)	5.43790 (10)
b (Å)	14.1920 (5)	9.3302 (5)	10.1973 (3)	5.3239 (3)	14.6396 (5)
c (Å)	7.6489 (2)	14.0691 (8)	14.5606 (4)	21.0164 (11)	9.1039 (3)
β (°)	92.412 (3)	99.281 (5)	90.072 (2)	102.510 (6)	92.003 (2)
V (Å^3)	571.75 (3)	1165.58 (11)	1517.45 (8)	1884.3 (2)	724.31 (4)
Z	2	4	4	4	2
D_{calcd} (g/cm^3)	3.608	4.543	3.728	3.934	4.630
λ (Å)	0.71073	0.71073	0.71073	0.71073	0.71073
μ (mm^{-1})	5.115	21.814	10.216	8.358	24.375
GOF [a]	1.056	1.057	1.062	1.045	1.072
R_1 [b]	0.0205	0.0273	0.0269	0.0214	0.0429
wR_2 [c]	0.0427	0.0665	0.0563	0.0463	0.1305

[a] GOF = $[\Sigma w(F_o^2 - F_c^2)^2/(N_o - N_p)]^{1/2}$, where N_o = no. of reflns and N_p = no. of refined parameters. [b] $R_1 = \Sigma||F_o| - |F_c||/\Sigma|F_o|$. [c] $wR_2 = [\Sigma w(F_o^2 - F_c^2)^2/\Sigma(w(F_o^2)^2]^{1/2}$.

The crystal structures of XeF_5AF_6 (A = Nb, Ta, Ru, Ir, Pt, Sb) are isotypic. The crystal structures of XeF_5AsF_6 and XeF_5AuF_6 are also isotypic, but differ from the previous structures. The crystal structure of XeF_5RhF_6 is a unique representative of a new type of structure. Some geometric parameters of the XeF_5AF_6 salts are listed in Tables 3 and 4.

Table 3. Geometric parameters (Å) of the $[XeF_5]^+$ cations, secondary Xe···F contacts (Å), and A–F bond lengths (Å) in the crystal structures of isotypic XeF_5AF_6 (A = Nb, Ta, Ru, Ir, Pt, Au) and literature data for XeF_5SbF_6.

	Nb [a]	**Ta** [a]	**Ru** [a]	**Ir** [a]	**Pt** [a]	**Sb** [b]
	Orthorhombic *Pnma*					
	150 K	**150 K**	**150 K**	**150 K**	**150 K**	**150 K**
$Xe–F_{ax}$	1.808 (3)	1.803 (7)	1.807 (3)	1.809 (5)	1.809 (5)	1.804 (3)
$Xe–F_{eq}$	1.839 (2)	1.839 (5)	1.843 (2)	1.835 (3)	1.838 (3)	1.841 (2)
	1.839 (2)	1.839 (5)	1.843 (2)	1.835 (3)	1.838 (3)	1.841 (2)
	1.842 (2)	1.843 (5)	1.846 (2)	1.843 (3)	1.839 (3)	1.844 (2)
	1.842 (2)	1.843 (5)	1.846 (2)	1.843 (3)	1.839 (3)	1.844 (2)
Xe···F	2.540 (3)	2.562 (6)	2.562 (3)	2.602 (5)	2.604 (5)	2.617 (3)
	2.535 (2)	2.560 (6)	2.587 (3)	2.616 (4)	2.646 (4)	2.638 (3)
	2.887 (2)	2.894 (5)	2.856 (2)	2.822 (3)	2.817 (3)	2.860 (2)
	2.887 (2)	2.894 (5)	2.857 (3)	2.822 (3)	2.817 (3)	2.860 (2)
A–F	1.835 (3)	1.849 (7)	1.820 (3)	1.841 (5)	1.857 (4)	1.857 (3)
	1.852 (3)	1.873 (7)	1.823 (3)	1.861 (5)	1.871 (4)	1.859 (3)
	1.886 (2)	1.880 (5)	1.854 (3)	1.879 (3)	1.884 (3)	1.882 (2)
	1.886 (2)	1.880 (5)	1.854 (3)	1.879 (3)	1.884 (3)	1.882 (2)
	1.925 (3)	1.930 (6)	1.878 (3)	1.892 (4)	1.894 (4)	1.895 (3)
	1.941 (3)	1.939 (6)	1.885 (3)	1.906 (5)	1.897 (4)	1.898 (3)

[a] This work. [b] Ref. [25].

Table 4. Geometric parameters (Å) of the $[XeF_5]^+$ cations, secondary Xe···F contacts (Å), and A–F bond lengths (Å) in the crystal structures of XeF_5AF_6 (A = Rh, Au) and literature data for XeF_5AsF_6 (monoclinic and orthorhombic phase).

	Rh [a]	**Au** [a]	**As** [b]	**As** [c]
	Orthorhombic *Pbca*	**Monoclinic $P2_1/c$**	**Monoclinic $P2_1/c$**	**Orthorhombic *Ama2***
	150 K	**150 K**	**150 K**	**100 K**
				Xe (2)/Xe (1)
$Xe–F_{ax}$	1.814 (2)	1.804 (5)	1.794 (3)	1.815 (7)/1.800 (8)
$Xe–F_{eq}$	1.833 (2)	1.823 (6)	1.826 (3)	1.844 (5)/1.840 (6)
	1.841 (2)	1.834 (6)	1.828 (3)	1.833 (8)/1.838 (6)
	1.842 (2)	1.835 (5)	1.833 (3)	1.833 (8)/1.838 (6)
	1.842 (2)	1.836 (5)	1.836 (3)	1.832 (8)/1.840 (6)
Xe···F	2.603 (2)	2.575 (6)	2.643 (3)	2.705 (5)/2.615 (6)
	2.664 (2)	2.746 (5)	2.722 (3)	2.705 (5)/2.615 (6)
	2.761 (2)	2.785 (6)	2.782 (3)	2.767 (6)/2.796 (6)
	2.844 (2)			2.767 (6)/3.451 (7)
				As (2)/As (1)
A–F	1.871 (2)	1.872 (6)	1.688 (3)	1.709 (5)/1.657 (7)
	1.873 (2)	1.876 (5)	1.696 (3)	1.709 (5)/1.657 (7)
	1.874 (2)	1.884 (5)	1.696 (3)	1.741 (6)/1.699 (6)
	1.879 (2)	1.903 (5)	1.738 (3)	1.749 (5)/1.699 (6)
	1.799 (2)	1.910 (5)	1.744 (3)	1.749 (5)/1.712 (6)
	1.815 (2)	1.911 (5)	1.750 (3)	1.710 (7)/1.712 (6)

[a] This work. [b] Ref. [37]. [c] Ref. [53].

The crystal structures of $XeF_5Nb_2F_{11}$ and $XeF_5Ta_2F_{11}$ are not isotypic and they also differ from the previously known crystal structure of $XeF_5Sb_2F_{11}$ [25]. Some geometric parameters are listed in Table 5.

Table 5. Geometric parameters (Å) of the $[XeF_5]^+$ cations, secondary Xe···F contacts (Å), and A–F (A = Nb, Ta) bond lengths (Å) and A–F_b–A angles (°) in the crystal structures of $XeF_5A_2F_{11}$ (A = Nb, Ta) and literature data for $XeF_5Sb_2F_{11}$.

	Nb [a]	**Ta** [a]	**Sb** [b]
	Monoclinic $P2_1$	**Monoclinic $I2/a$**	**Triclinic $P\bar{1}$**
	150 K	**150 K**	**200 K**
Xe–F_{ax}	1.801 (3)	1.802 (6)	1.883 (3)
Xe–F_{eq}	1.826 (3)	1.838 (3)	2.019 (3)
	1.836 (3)	1.838 (3)	2.029 (3)
	1.837 (3)	1.839 (4)	1.837 (3)
	1.838 (4)	1.839 (4)	1.838 (3)
Xe···F	2.582 (3)	2.666 (4)	2.915 (3)
	2.633 (3)	2.872 (3)	2.848 (3)
	2.667 (3)	2.872 (3)	2.775 (3)
			2.814 (3)
A (1)–F_t	1.823 (3)	1.824 (4)	1.838 (3)
	1.840 (4)	1.849 (4)	1.846 (3)
	1.846 (4)	1.855 (4)	1.853 (3)
	1.847 (4)	1.900 (4)	1.866 (3)
	1.918 (3)	1.910 (4)	1.883 (3)
A (1)–F_b	2.096 (3)	2.0657 (6)	2.019 (3)
		2.0657 (6)	
A (2)–F_t	1.821 (4)		1.837 (3)
	1.832 (3)		1.838 (3)
	1.833 (4)		1.843 (3)
	1.910 (3)		1.870 (3)
	1.923 (3)		1.878 (3)
A (2)–F_b	2.038 (3)		2.029 (3)
A–F_b–A	155.63 (19)	169.6 (3)	145.09 (16)

[a] This work. [b] Ref. [25].

The crystal structure of $XeF_5Ni(AsF_6)_3$ is isotypical to the previously reported crystal structures of $XeF_5M(SbF_6)_3$ (M^{2+} = Mg, Mn, Co, Ni, Cu, Zn, Pd) [34,35]. Some geometric parameters are given in Table 6.

Table 6. Experimental geometric parameters (Å) of the two crystallographically independent Ni^+ cations, geometric parameters (Å) of the $[XeF_5]^+$ cations, and secondary Xe···F contacts in the crystal structures of $XeF_5Ni(AsF_6)_3$ and literature data for $XeF_5Ni(SbF_6)_3$.

	$XeF_5Ni(AsF_6)_3$ [a]	**$XeF_5Ni(SbF_6)_3$** [b]
	$P2_1/n$	
	150 K	
Ni (1)–F	2.000 (2)	2.002 (1)
	2.000 (2)	2.002 (1)
	1.994 (2)	1.989 (1)
	1.994 (2)	1.989 (1)
	2.006 (2)	2.013 (1)
	2.006 (2)	2.013 (1)

Table 6. *Cont.*

	$XeF_5Ni(AsF_6)_3$ [a]	$XeF_5Ni(SbF_6)_3$ [b]
	$P2_1/n$	
	150 K	
Ni (2)–F	1.999 (2)	1.991 (1)
	1.999 (2)	1.991 (1)
	2.006 (2)	1.979 (1)
	2.006 (2)	1.979 (1)
	2.010 (2)	2.006 (1)
	2.010 (2)	2.006 (1)
$Xe–F_{ax}$	1.782 (2)	1.800 (2)
$Xe–F_{eq}$	1.818 (2)	1.825 (2)
	1.819 (2)	1.828 (2)
	1.820 (2)	1.826 (2)
	1.822 (2)	1.832 (2)
Xe···F	2.903 (2)	2.866 (2)
	2.919 (3)	2.928 (2)
	2.931 (2)	2.944 (2)
	2.971 (3)	2.898 (2)

[a] This work. [b] Ref. [35].

The crystal structure of $[Ni(XeF_2)_2](IrF_6)_2$ is isotypical of crystal structure of $[Cu(XeF_2)_2](SbF_6)_2$ reported previously [54]. Some geometric parameters are listed in Table 7.

Table 7. Experimental geometric parameters (Å) in the crystal structure of $[Ni(XeF_2)_2](IrF_6)_2$ and literature data for $[Cu(XeF_2)_2](SbF_6)_2$.

	$[Ni(XeF_2)_2](IrF_6)_2$ [a]	$[Cu(XeF_2)_2](SbF_6)_2$ [b]
	$P2_1/c$	
	150 K	200 K
$M–F_b$ (AF_6)	2.016 (6)	2.090 (5)
	2.016 (6)	2.090 (5)
	2.023 (7)	2.123 (5)
	2.023 (7)	2.123 (5)
$M–F_b$ (XeF_2)	1.938 (6)	1.857 (5)
	1.938 (6)	1.857 (5)
$Xe–F_t$	1.920 (7)	1.906 (5)
$Xe–F_b$	2.078 (6)	2.102 (5)
$A–F_b$	1.921 (7)	1.891 (5)
	1.934 (7)	1.917 (5)
$A–F_t$	1.843 (8)	1.841 (6)
	1.852 (8)	1.843 (6)
	1.858 (8)	1.861 (6)
	1.861 (8)	1.870 (6)

[a] This work. [b] Ref. [54].

3. Discussion

3.1. Crystal Structures of XeF_5AF_6 (A = Nb, Ta, Ru, Rh, Os, Ir, Pt, Au, As, Sb)

Prior to this study, the crystal structures of XeF_5NbF_5 (293 K) [30], XeF_5RuF_5 (RT; room temperature) [38], XeF_5PtF_5 (RT) [24], XeF_5AuF_5 (RT) [39], XeF_5AsF_6 (80 K, 100 K, 150 K, 298 K) [37,41,53], XeF_5SbF_6 (150 K, 296 K) [25,37], and mixed anion $[XeF_5][As_{0.3}Sb_{0.7}F_6]$ (200 K, 295 K) and $[XeF_5][As_{0.5}Sb_{0.5}F_6]$ (150 K, 295 K) salts [37] were known. X-ray powder diffraction (XPD) images showed that XeF_5AF_6 (A = Os, Ir, Pt, and Ru) are isotypic [39].

The crystal structures of XeF_5AF_5 (A = Nb, Ru, Pt, Au) determined at 150 K are the same as at room temperature. The crystal structure of XeF_5IrF_5 agrees with the XPD data [39], while the crystal structures of XeF_5TaF_6 and XeF_5RhF_6 have been determined for

the first time. Based on the results of this study and the data known from the literature, the crystal structures of the XeF_5AF_6 salts (A = Nb, Ta, Ru, Rh, Os, Ir, Pt, Au, As, Sb) can be classified into four types of structures (type I, II, III, and IV).

3.1.1. Type I; XeF_5AF_6 (A = Nb, Ta, Ru, Os, Ir, Pt, Sb) Salts

The crystal structure of XeF_5PtF_6 was described as the first example of type I [24]. The crystal structures of the salt XeF_5AF_6 (A = Nb, Ta, Ru, Os, Ir, Sb) are isotypic to this type (Tables 1 and 3). The members of type I crystallize in the orthorhombic Pnma space group, in which the asymmetric structural unit consists of a crystallographically unique $[XeF_5]^+$ cation and $[AF_6]^-$ anion (Figure 1).

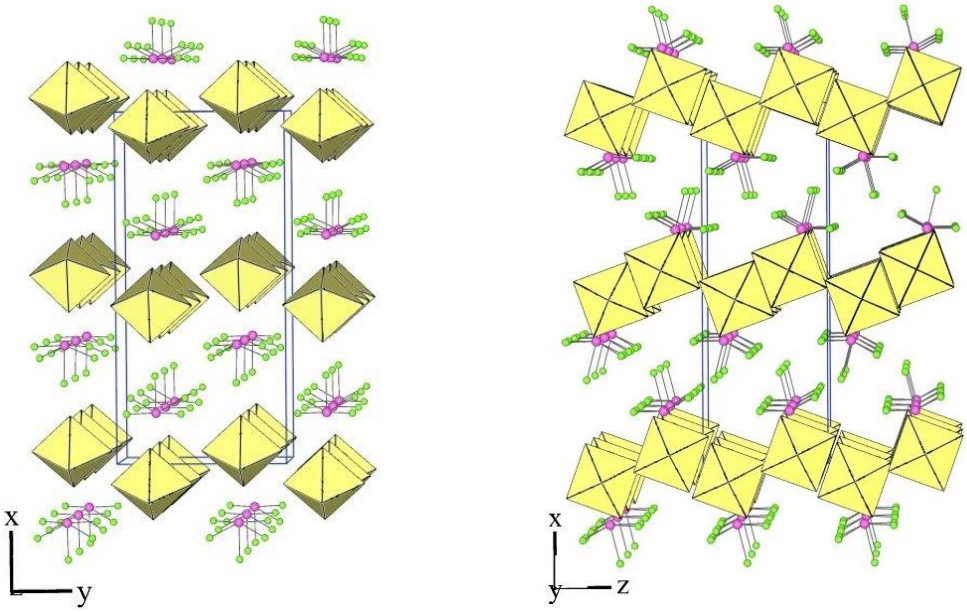

Figure 1. Two different views of the packing of $[XeF_5]^+$ cations and $[IrF_6]^-$ anions in the crystal structure of $[XeF_5][IrF_6]$ (type I).

Each $[XeF_5]^+$ cation exhibits the typical geometry, i.e., a pseudo-octahedral AX_5E VSEPR arrangement of the bond pairs (X) and the lone pair (E). The Xe–F_{ax} bonds are shorter than the other four Xe–F_{eq} distances (Table 4, Figure 2). Each XeF_5 unit forms four secondary contacts with the fluorine atoms of four AF_6 groups (Figure 2). Each $[AF_6]^-$ anion participates in four secondary contacts with four different XeF_5 groups (Figure 2).

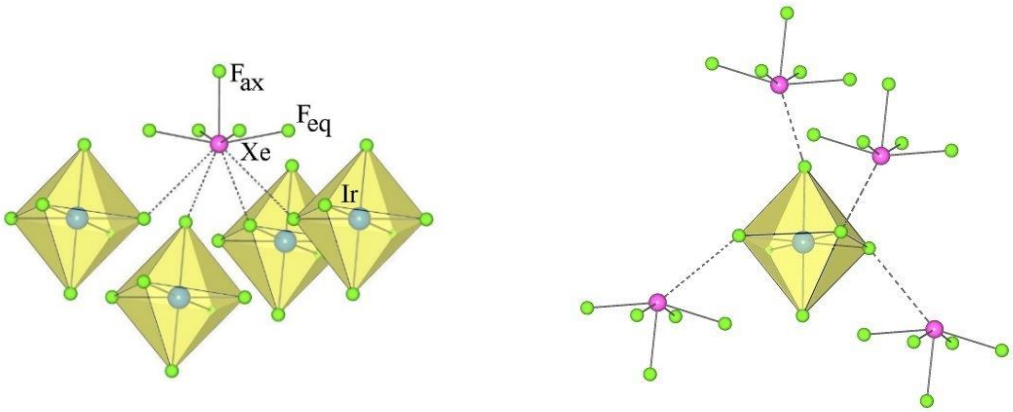

Figure 2. Secondary contacts between the $[XeF_5]^+$ cations and $[IrF_6]^-$ anions in the crystal structure of $[XeF_5][IrF_6]$ (type I).

3.1.2. Type II; XeF_5AF_5 (A = As, Au) Salts

The crystal structures of XeF_5AuF_6 and the monoclinic form of XeF_5AsF_6 are examples of type II (Tables 1 and 4). They crystallize in the monoclinic space group $P2_1/c$. The asymmetric structural unit of type II consists of a crystallographically equivalent $[XeF_5]^+$ cation and an $[AF_6]^-$ anion (Figure 3).

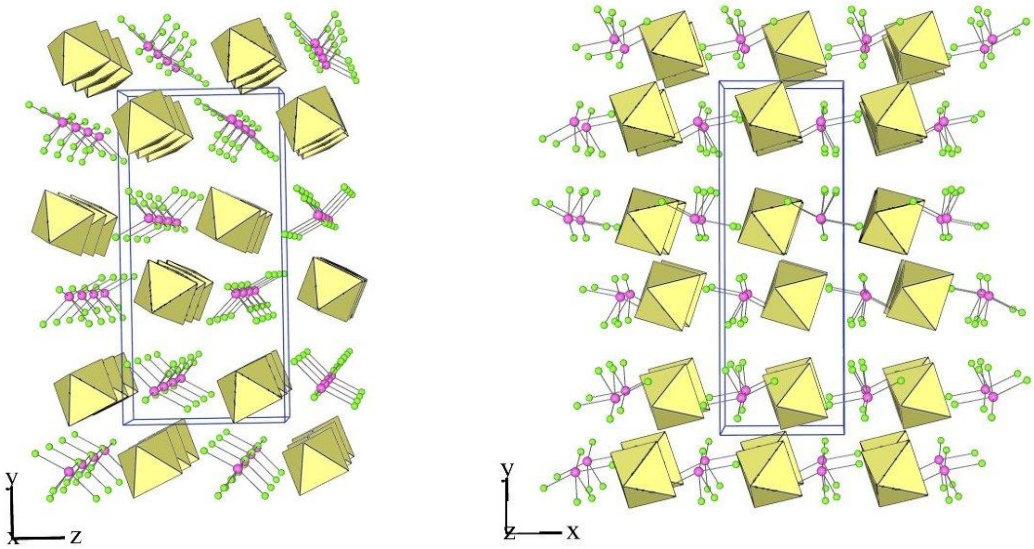

Figure 3. Two different views of the packing of $[XeF_5]^+$ cations and $[AuF_6]^-$ anions in the crystal structure of $[XeF_5][AuF_6]$ (type II).

The geometry of the $[XeF_5]^+$ in the salts of type II is the same as in type I [d(Xe–F_{ax}) < d(Xe–F_{eq}); Table 4, Figure 4), while the number of secondary contacts between $[XeF_5]^+$ cations and $[AF_6]^-$ anions is different. In type II, each $[XeF_5]^+$ cation forms three secondary contacts with the fluorine atoms of two AF_6 groups and each $[AF_6]^-$ anion participates in three secondary contacts with two different XeF_5 groups (Figure 4).

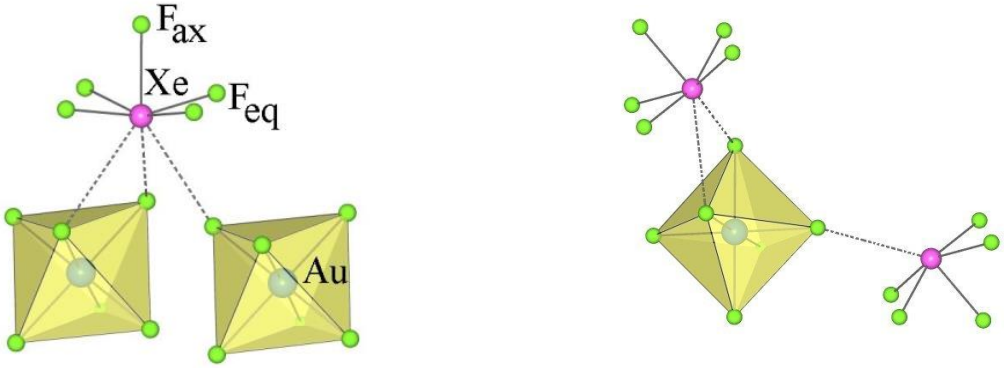

Figure 4. Secondary contacts between the $[XeF_5]^+$ cations and $[AuF_6]^-$ anions in the crystal structure of $[XeF_5][AuF_6]$ (type II).

3.1.3. Type III; XeF_5AF_5 (A = Rh) Salts

The crystal structure of XeF_5RhF_6 is the only representative of type III (Tables 1 and 4). It crystallizes in the orthorhombic space group *Pbca*. The asymmetric structural unit of type III consists of a crystallographically equivalent $[XeF_5]^+$ cation and an $[AF_6]^-$ anion (Figure 5).

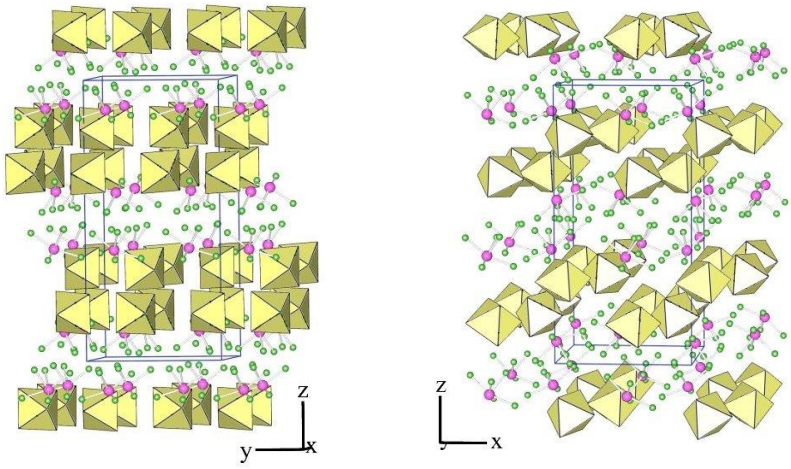

Figure 5. Two different views of the packing of $[XeF_5]^+$ cations and $[RhF_6]^-$ anions in the crystal structure of $[XeF_5][RhF_6]$ (type III).

The geometry of the $[XeF_5]^+$ in the type III salts is similar to that in the type I and II compounds (d(Xe–F_{ax}) < d(Xe–F_{eq}); Table 4, Figure 6), while the nature of the secondary interaction contacts between the $[XeF_5]^+$ cations and the $[AF_6]^-$ anions is different. In type III, each $[XeF_5]^+$ cation forms four secondary contacts with the fluorine atoms of three AF_6 groups, while each $[AF_6]^-$ anion participates in four secondary contacts with three different XeF_5 groups (Figure 6).

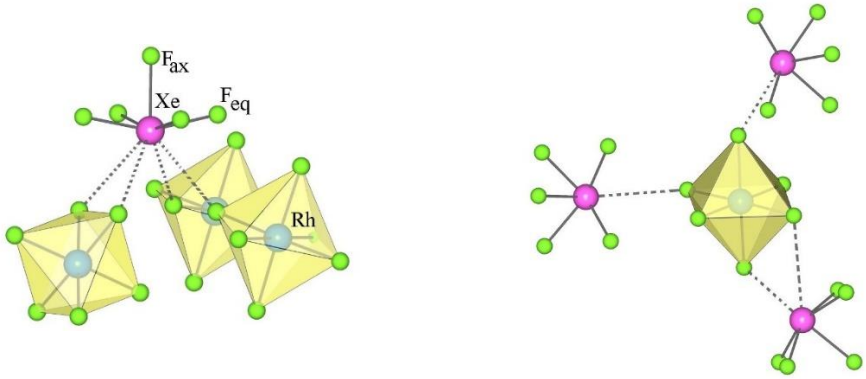

Figure 6. Secondary contacts between the $[XeF_5]^+$ cations and $[RhF_6]^-$ anions in the crystal structure of $[XeF_5][RhF_6]$ (type III).

3.1.4. Type IV; Orthorhombic XeF_5AsF_6 and Mixed Anionic $[XeF_5][As_{0.3}Sb_{0.7}F_6)$ and $[XeF_5][As_{0.5}Sb_{0.5}F_6)$ Salts

The crystal structure of XeF_5AsF_6 was first determined at room temperature [41] and later redetermined at 150 K [37]. When the crystal first measured at 150 K was cooled to 80 K and data were collected, no phase transition was observed [37]. In both cases, only a monoclinic phase was obtained (150 K; $P2_1/c$, Z = 4, a = 5.8222 (6) Å, b = 16.3566 (15) Å, c = 7.9247 (8) Å, β = 90.729 (9) °). However, single crystals of orthorhombic XeF_5AsF_6 (Table 8) crystallized from aHF solution between 22 and −30 °C [53]. The corresponding aHF solution was prepared by redox decomposition of $[FKrFXeF][AsF_6]\cdot 0.5KrF_2\cdot 2HF$ heated stepwise and four different times, from −65 °C to 22 °C. The asymmetric structural unit consists of two crystallographically nonequivalent $[XeF_5]^+$ cations and two $[AsF_6]^-$ anions [53].

Table 8. Summary of crystal data for the orthorhombic XeF_5AsF_6 and mixed anion $[XeF_5][As_{0.3}Sb_{0.7}F_6]$ and $[XeF_5][As_{0.5}Sb_{0.5}F_6]$ salts.

Compound	Crystal System	Space Group	*Z*	*a* /Å	*b* /Å	*c* /Å	*T* /K
XeF_5AsF_6 [a]	orthorhombic	*Ama*2	8	9.796 (2)	13.272 (10)	11.578 (2)	100
$[XeF_5][As_{0.3}Sb_{0.7}F_6]$ [b]	orthorhombic	*Ama2(00γ)s0s*	8	10.031 (1)	13.362 (1)	11.808 (1)	200
β-$[XeF_5][As_{0.5}Sb_{0.5}F_6]$ [b]	orthorhombic	*Ama2(00γ)s0s*	8	10.1196 (5)	13.4517 (6)	11.8999 (5)	295
α-$[XeF_5][As_{0.5}Sb_{0.5}F_6]$ [b]	orthorhombic	$Pca2_1$	16	9.9738 (2)	13.2492 (4)	23.3701 (7)	150

[a] Ref. [53]. [b] Ref. [37].

Similar unit cell parameters (Table 8) were determined for orthorhombic $[XeF_5][As_{0.3}Sb_{0.7}F_6]$ (100–295 K) and *β*-$[XeF_5][As_{0.5}Sb_{0.5}F_6]$ (295 K), both of which have a (3 + 1)-dimensional incommensurately modulated crystal structure (superspace group *Ama2(00γ)s0s*) [37]. At 150 K, the *α*-$[XeF_5][As_{0.5}Sb_{0.5}F_6]$ salt is also orthorhombic, but not modulated (space group $Pca2_1$) and with doubled *c*-axis (Table 8) [37]. In $[XeF_5][As_{0.3}Sb_{0.7}F_6]$ and *β*-$[XeF_5][As_{0.5}Sb_{0.5}F_6]$ there are two crystallographically nonequivalent $[XeF_5]^+$ cations and two crystallographically independent sites for pnictogen atoms, while in *α*-$[XeF_5][As_{0.5}Sb_{0.5}F_6]$ there are four crystallographically nonequivalent $[XeF_5]^+$ cations and four crystallographically different sites for pnictogen atoms.

All the compounds listed in Table 8 are structurally related, as indicated by the similar packing in their crystal structures (Figure 7). It is practically identical in the orthorhombic XeF_5AsF_6, $[XeF_5][As_{0.3}Sb_{0.7}F_6]$, and *β*-$[XeF_5][As_{0.5}Sb_{0.5}F_6]$ and slightly different in *α*-$[XeF_5][As_{0.5}Sb_{0.5}F_6]$ due to the different inclination of some AF_6 (A = As, Sb)octahedra.

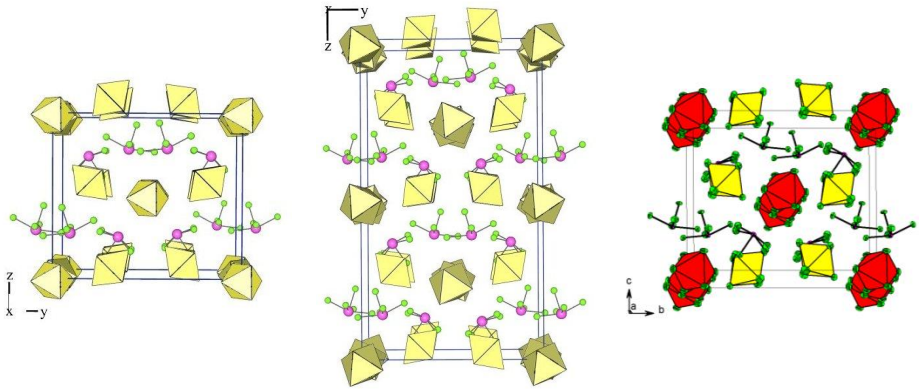

(**a**) (**b**) (**c**)

Figure 7. Packing of $[XeF_5]^+$ cations and $[AF_6]^-$ anions (A = As, Sb) in the crystal structures of (**a**) orthorhombic $[XeF_5][AsF_6]$; (**b**) *α*-$[XeF_5][As_{0.5}Sb_{0.5}F_6]$; (**c**) average structure of $[XeF_5][As_{0.3}Sb_{0.7}F_6]$. The last figure is reproduced from Ref. [37] and published under the terms and conditions of the Creative Commons Attribution 4.0 International License CC BY 4.0.

In the orthorhombic $[XeF_5][AsF_6]$ [53] each $[Xe(1)F_5]^+$ cation forms three shorter (<3 Å) and one longer secondary contact (3.451 (7) Å) with the fluorine atoms of four AsF_6 groups. The sum of the Xe···F van der Waals radii is 3.63 Å [55]. The other $[Xe(2)F_5]^+$ cation is also involved in four secondary interactions (<3 Å), but only with three AsF_6 groups. Each $[As(1)F_6]^-$ anion interacts with four $[XeF_5]^+$ cations and each $[As(2)F_6]^-$ anion interacts with only three $[XeF_5]^+$ cations (Figure 8).

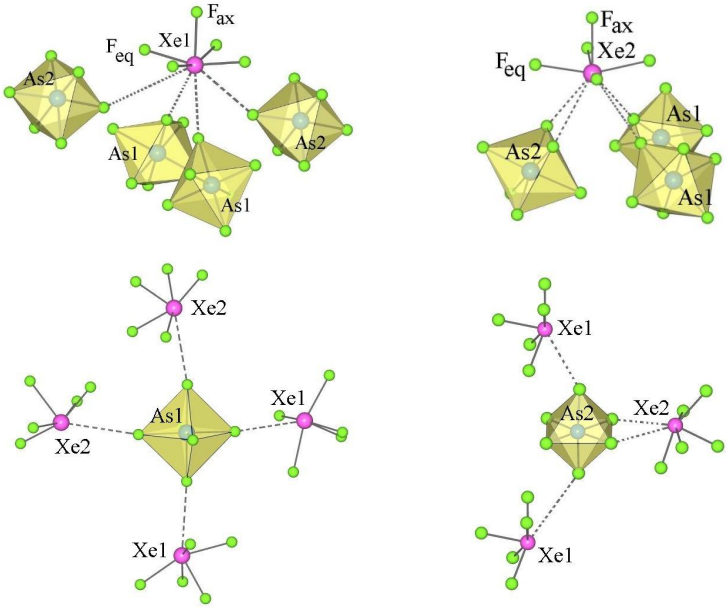

Figure 8. Secondary contacts between the $[XeF_5]^+$ cations and the $[AsF_6]^-$ anions in the crystal structure of orthorhombic $[XeF_5][AsF_6]$ (type IV).

In α-$[XeF_5][As_{0.5}Sb_{0.5}F_6]$ [37], the cations $[Xe(1)F_5]^+$ and $[Xe(2)F_5]^+$ each form four secondary contacts (<3 Å) with the fluorine atoms of three AF_6 groups (A = As, Sb), while $[Xe(3)F_5]^+$ and $[Xe(4)F_5]^+$ have three shorter (<3 Å) and one longer (3.437(7) Å and 3.420(7) Å, respectively) contact with four AF_6 groups (Figure 9). Each of the crystallographically unique $[A(1)F_6]^-$ and $[A(2)F_6]^-$ anions forms four interactions with three $[XeF_5]^+$ cations, while the $[A(3)F_6]^-$ and $[A(4)F_6]^-$ anions form four interactions with four $[XeF_5]^+$ cations, (Figure 10).

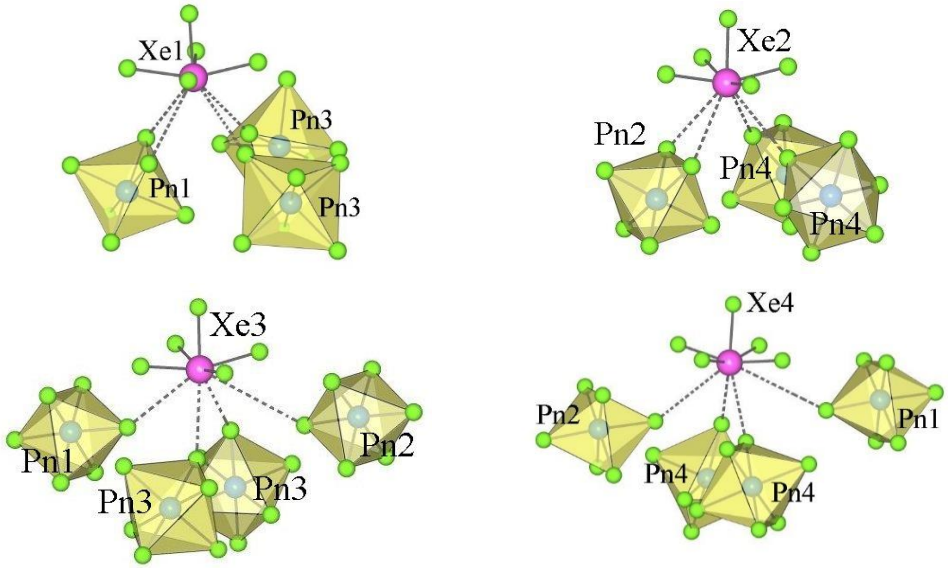

Figure 9. Secondary contacts between the $[XeF_5]^+$ cations and the surrounding $[AF_6]^-$ anions (A = As, Sb) in the crystal structure of α-$[XeF_5][As_{0.5}Sb_{0.5}F_6]$.

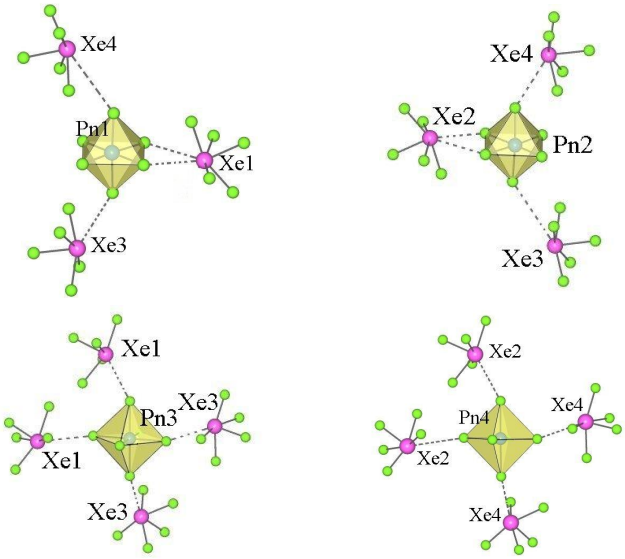

Figure 10. Secondary contacts between the $[AF_6]^-$ (A = As, Sb) anions and the surrounding $[XeF_5]^+$ cations in the crystal structure of α-$[XeF_5][As_{0.5}Sb_{0.5}F_6]$.

3.1.5. General Considerations for XeF_5AF_6 Salts (A = Nb, Ta, Ru, Rh, Os, Ir, Pt, Au, As, Sb)

Table 9 lists the effective ionic radii $r(A^{5+})$ (A = Nb, Ta, Ru, Rh, Os, Ir, Pt, Au, As, Sb) for coordination number six [56], the formula units (molecular) volumes V_{FU} of $LiAF_6$, $CsAF_6$, and XeF_5AF_6, and the average A–F bond lengths in $LiAF_6$ and XeF_5AF_6. The molecular volumes of $LiAF_6$, $CsAF_6$, and XeF_5AF_6 are shown in Figure 11. The crystal structures of $LiAF_6$ (A = Nb, Ta, Ru, Rh, Os, Ir, Pt, and Au) were determined by synchrotron X-ray powder diffraction at 299 K [57]. The crystal structures of $LiAsF_6$ and $LiSbF_6$ were determined by X-ray diffraction on powdered material and single crystals, respectively, at room temperature (RT) [58,59]. With the exception of $CsAsF_6$ and $CsSbF_6$, whose complete crystal structures were determined on single crystals at RT, only unit cells determined at RT are available for the other $CsAF_6$ salts [60]. The crystal structures of $CsAF_6$ (A = Rh, Pt, Ir, Os, and Au) were also determined on single crystals at 150 K [61]. The crystal structures of XeF_5AF_6 (A = Nb, Ta, Ru, Rh, Ir, Pt, Au, As [37], Sb [25]) were determined at 150 K and some of them also at RT (A = As [41], Au [39], Pt [24], Ru [38], Sb [37], Nb [30]).

Table 9. Effective ionic radii $r(A^{5+})$ (A = Nb, Ta, Ru, Rh, Os, Ir, Pt, Au, As, Sb) for coordination number six (Å), formula unit (molecular) volumes V_{FU} (Å^3) of $LiAF_6$, $CsAF_6$, and XeF_5AF_6, and average A–F bond lengths d_{av}[A–F] (Å) in $LiAF_6$ and XeF_5AF_6.

A	**As**	**Rh**	**Au**	**Pt**	**Ir**	**Ru**	**Os**	**Sb**	**Nb**	**Ta**
$r(A^{5+})$ [a]	0.46	0.55	0.57	0.57	0.57	0.565	0.575	0.60	0.64	0.64
$LiAF_6$										
V_{FU}	94.6 [b]	98.64 [c]	99.12 [c]	99.61 [c]	100.77 [c]	100.5 [c]	102.41 [c]	105.3 [d]	110.92 [c]	111.26 [c]
d_{av}[A–F]	1.74	1.855	1.874	1.887	1.879	1.851	1.872	1.877	1.863	1.859
$CsAF_6$										
V_{FU} [e]	138.6	141.2	138.95	143.4	143.6	141.7	144.5	149	147.9	149.3
V_{FU} [f]		137.07		138.42	138.97	138.35	139.97			
XeF_5AF_6										
Type	II	III	II	I	I	I	I	I	I	I
V_{FU} [g]	196.15		203.03	196.35	194.34	193.26		199.42	200	
V_{FU} [h]	188.67	181.18	195.71	190.15	190.18	188.62		195.11	194.33	195.85
d_{av}[A–F]	1.719	1.852	1.893	1.881	1.876	1.852		1.879	1.888	1.892

[a] Ref. [56]. [b] Room temperature (RT); Ref. [58]. [c] 299 K; Ref. [57]. [d] RT; Ref. [59]. [e] RT; Ref. [60]. [f] 150 K; Ref. [61]. [g] 285 K for Ir salt (this work); others RT (Refs. [24,30,37–39,41]). [h] This work (150 K) except XeF_5AsF_6 (150 K) [37] and XeF_5SbF_6 (150 K) [25].

Although the formula unit volumes V_{FU} of the $LiAF_6$ and $CsAF_6$ salts (Figure 11) show a similar trend, this is not the case for the XeF_5AF_6 salts, with the V_{FU} of XeF_5RhF_6 and XeF_5AuF_6 being particularly prominent. For $LiAF_6$ and $CsAF_6$, the V_{FU} are smallest for the As, Rh, and Au salts and largest for the Sb, Nb, and Ta salts. For the $[XeF_5]^+$ salts, the V_{FU} of XeF_5AuF_6 is almost identical to the V_{FU} of XeF_5TaF_6, while XeF_5RhF_6 has the smallest value V_{FU} of all XeF_5AF_6 salts (Table 9, Figure 11).

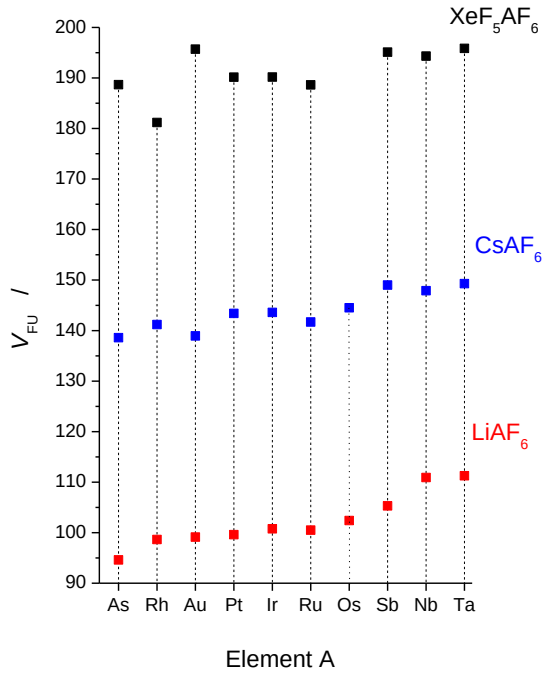

Figure 11. Formula unit volumes of $LiAF_6$ (for A = Rh, Au, Pt, Ir, Ru, Os, Nb, Ta at 299 K and for A = As, Sb at room temperature), $CsAF_6$ (all data at room temperature), and XeF_5AF_6 salts (all data at 150 K).

3.2. Crystal Structures of $XeF_5A_2F_{11}$ (A = Nb, Ta, Sb)

In the XeF_6–AF_5 (A = Nb, Ta) system, only the salts XeF_5AF_6 and $Xe_2F_{11}AF_6$ have been known so far [30,62,63]. The salts $XeF_5Nb_2F_{11}$ and $XeF_5Ta_2F_{11}$ were prepared for the first time in this study. As in the case of $XeF_5Sb_2F_{11}$ [25] (Figure 12) the crystal structures of $XeF_5A_2F_{11}$ (A = Nb, Ta) consist of discrete $[XeF_5]^+$ cations and dimeric $[A_2F_{11}]^-$ anions interacting through secondary fluorine bridge Xe···F–A contacts (Figures 13 and 14). Each crystal structure of the $XeF_5A_2F_{11}$ salts (A = Sb, Nb, Ta) represents a unique example (Tables 2 and 5).

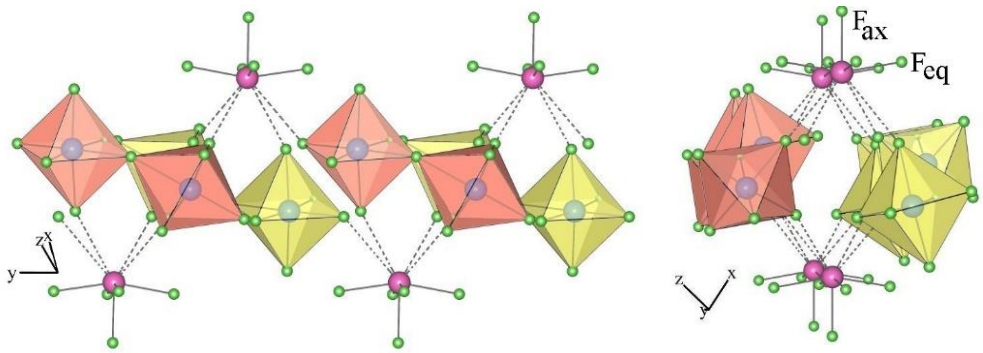

Figure 12. Secondary contacts between the $[XeF_5]^+$ cations and the $[Sb_2F_{11}]^-$ anions in the crystal structure of $XeF_5Sb_2F_{11}$.

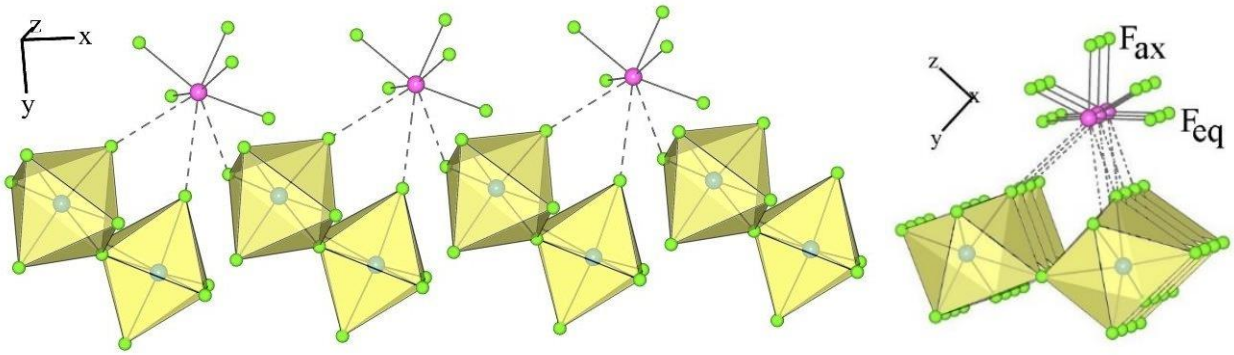

Figure 13. Secondary contacts between the $[XeF_5]^+$ cations and the $[Nb_2F_{11}]^-$ anions in the crystal structure of $XeF_5Nb_2F_{11}$.

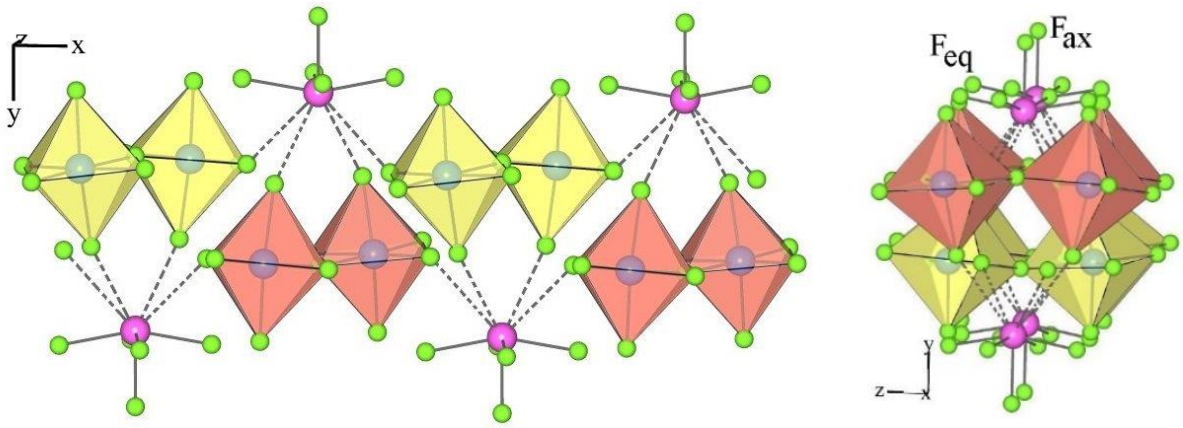

Figure 14. Secondary contacts between the $[XeF_5]^+$ cations and the $[Ta_2F_{11}]^-$ anions in the crystal structure of $XeF_5Ta_2F_{11}$.

In $XeF_5Nb_2F_{11}$, each $[XeF_5]^+$ cation forms three secondary contacts with the fluorine atoms of two Nb_2F_{11} groups, whereas in $XeF_5Sb_2F_{11}$ and $XeF_5Ta_2F_{11}$, each $[A_2F_{11}]^-$ anion (A = Nb, Ta) participates in four secondary contacts with three different A_2F_{11} dimers (Figures 12–14). In all three salts, the Xe–F_{ax} bonds are shorter than the other four Xe–F_{eq} distances (Table 5). The A–F_b–A bridge (Table 5) in the dimeric $[A_2F_{11}]^-$ anion (A = Sb, Nb, Ta) is not linear as in $[A_2F_{11}]^-$ (M = Nb, Ta) salts of protonated 1,3-dimethoxybenzene but bent as in many other examples [64]. In $XeF_5Sb_2F_{11}$, the four F_{eq} atoms of the $Sb(1)F_6$ unit are in staggered position in respect to the four F_{eq} of the $Sb(2)F_6$ group with a torsion angle of ~37.5°, while in the corresponding Nb and Ta salts they are almost in an eclipsed position.

3.3. Crystal Structure of $XeF_5Ni(AsF_6)_3$

The crystal structure of $XeF_5Ni(AsF_6)_3$ (Figure 15) is isotypical to the crystal structure of $XeF_5Ni(SbF_6)_3$ [35]. The cation Ni^{2+} is coordinated by six fluorine atoms provided by six octahedral anions $[AsF_6]^-$ forming almost regular NiF_6 octahedra. The Ni−F bond lengths in both salts are virtually identical (Table 6). They range from 1.989 (1) to 2.013 (1) Å. Due to the sharing of fluorine atoms, the NiF_6 and AsF_6 octahedra are connected to form a three-dimensional framework. The $[XeF_5]^+$ cations are located inside the cavities. The geometry of the $[XeF_5]^+$ cations is almost identical in both Ni salts (Table 5).

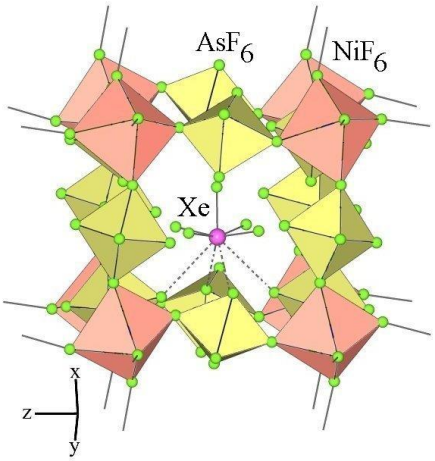

Figure 15. Part of the crystal structure of $XeF_5Ni(AsF_6)_3$.

3.4. Crystal Structures of the Salts $(Xe_2F_{11})_2(NiF_6)_2$ and $Ni(XeF_2)_2(IrF_6)_2$

The crystal structure of $(Xe_2F_{11})_2(NiF_6)_2$ determined at 150 K is the same as that at room temperature [40], which means that there is no phase transition in the 150–296 K range.

It has been reported that the reaction between $M^{n+}(AF_6)_n^-$ and XeF_2 in anhydrous aHF (aHF) leads to coordination compounds $[M^{n+}(XeF_2)_p](AF_6)_n^-$ (where XeF_2 is coordinated to a metal cation M^{n+}) only when the Lewis acidity of M^{n+} is not high enough to withdraw F^- ions from XeF_2 to form MF_n and $Xe_2F_3^+AF_6^-$ [65]. Since the reaction between $Ni(AsF_6)_2$ and XeF_2 in aHF gave NiF_2 and $Xe_2F_3AsF_6$, the preparation of $[Ni(XeF_2)_2](IrF_6)_2$ was a small surprise.

The crystal structure of $[Ni(XeF_2)_2](IrF_6)_2$ is isotypical to the crystal structure of $[Cu(XeF_2)_2](SbF_6)_2$ [54]. In both structures, adjacent $[M(XeF_2)_2]^{2+}$ units are connected via two $[AF_6]^-$ units with bridging fluorine atoms in the cis position to form infinite chains that are parallel to the *x*–axis (Figure 16). These chains are interconnected by weak $F_2Xe\cdots F–AF_5$ contacts and form a three-dimensional network.

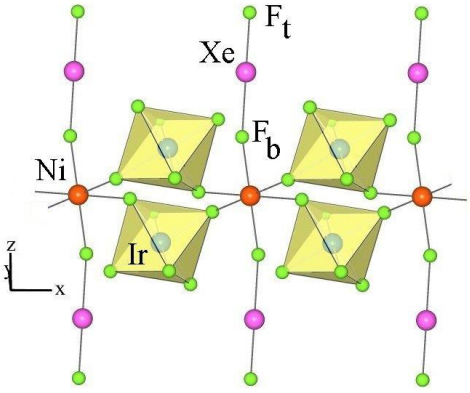

Figure 16. Part of the crystal structure of $[Ni(XeF_2)_2](IrF_6)_2$.

The metal cation Ni^{2+} is sixfold coordinated by fluorine atoms of two XeF_2 ligands and four $[IrF_6]^-$ anions. In $[Cu(XeF_2)_2](SbF_6)_2$, the Cu^{2+} cation is coordinated by two XeF_2 molecules (Cu–F = 2 × 1.857 (5) Å) and four fluorine atoms provided by four $[SbF_6]$ units with two shorter and two longer Cu–F bonds (2 × 2.090 (5) Å and 2 × 2.123 (5) Å) [54]. In contrast, the Ni–F(Ir) bonds in the $Ni(XeF_2)_2(IrF_6)_2$ salt are almost the same length (2 × 2.016 (9) Å and 2 × 2.023 (7) Å). The Ni–F(XeF_2) bonds are much longer (2 × 1.938(6) Å) than in the $[Cu(XeF_2)_2](SbF_6)_2$ salt (2 × 1.857 (5) Å), indicating a weaker M^{2+}–FXeF interaction in the Ni salt. Consequently, Xe–F_b (F_b = bridging F atom) is shorter (2.078 (6) Å) in the Ni salt than in the Cu salt (2.102 (5) Å) and the opposite is true for Xe−F_t bonds [F_t = terminal fluorine atom; 1.920 (7) Å (Ni salt) and 1.906 (5) Å (Cu salt)].

4. Materials and Methods

CAUTION: Anhydrous HF and some fluorides are highly toxic and must be handled under a well-ventilated hood, and protective clothing must be worn at all times!

4.1. Apparatus, Techniques, and Reagents

The handling of volatile (anhydrous HF, F_2, AsF_5, BF_3) and nonvolatile materials and the type of the reaction and crystallization vessels have already been reported [35,47,66]. Metallic Re powder (Alfa Aesar, Haverhill, MA, USA, 99.99%), Ru sponge (Alfa Aesar, 99.95%), Rh sponge (BDH, 99.9%), Os powder (Alfa Aesar, 99.8%), Ir sponge (Alfa Aesar, 99.95%), Pt powder (Aldrich, St. Louis, MO, USA, 99.9%), elemental F_2 (Solvay Fluor and Derivate GmbH, Hannover, Germany 99.98%), CrF_3 (Messer Griesheim, Bad Soden, Germany, 99.9%), and BF_3 (Union Carbide Austria, GmbH, 99.5%) were used as supplied. Anhydrous HF (Linde AG, Pullach, Germany, 99.995%) was treated with K_2NiF_6 (Advance Research Chemicals Inc, Catoosa, OK, USA, 99.9%) for several hours before use. NiF_2 (Alfa Products, Bedford Park, IL, USA, 99.5%) and CuF_2 (Aldrich, 98%) were treated with elemental F_2 at 220 °C for several hours before use. NbF_5 (Alfa Aesar, 99%) and TaF_5 (Alfa Aesar, 99.9%) were sublimed before use. AuF_3 [66], XeF_2 [67], AsF_5 [68], XeF_5SbF_6 [34], $Sn(SbF_6)_2$ [69,70], $Pb(SbF_6)_2$ [69,70], and $Zn(SbF_6)_2$ [69,70] were synthesized as described previously.

Raman spectra were recorded at room temperature using a Renishaw Raman Imaging Microscope System 1000 or a Horiba Jobin Yvon LabRam-HR spectrometer [66].

4.2. Attempted Preparation of $XeF_5M(AF_6)_3$ (M = Cu, Ni; A = Cr, Nb, Ta, Ru, Rh, Re, Os, Ir, Pt, Au, As), $XeF_5M(SbF_6)_3$ (M = Sn, Pb), and $XeF_5M(BF_4)_x(SbF_6)_{3-x}$ (x = 1, 2, 3; M = Co, Mn, Ni, Zn)

The solid starting reagents were loaded into reaction vessels in a dry box (Table S1). The solvent HF and optionally BF_3, AsF_5, and SbF_5 were condensed at 77 K to solid reagents, and the reaction vessel was warmed to ambient temperature. Fluorine was slowly added to the reaction vessel at room temperature. A medium-pressure mercury lamp (Hg arc lamp, 450 W, Ace Glass, Vineland, NJ, USA) was used as the UV source. After several days of intensive stirring at room temperature, the volatiles were pumped off and the Raman spectra of the obtained solids were recorded (Figures S1–S11).

For crystallization, the clear supernatant, which contained no visible sediment, was decanted into the side arm of the crystallization vessel, which consisted of two tubes made of fluoropolymer. Evaporation of the solvent from the side arm was achieved by maintaining a temperature gradient of about 10–20 °C between the two tubes for several weeks. Slow distillation of aHF resulted in crystal growth.

Crystals were immersed in perfluorodecalin (melting point 263 K) in a dry box, selected under the microscope, and mounted on the goniometer head of the diffractometer in a cold nitrogen stream (265–273 K). Some of them were sealed in quartz capillaries used to record Raman spectra at several random positions (Figures S1–S11).

4.3. Crystal Structure Determination

Single-crystal X-ray diffraction data of reported crystal structures were acquired at 150 K (for XeF_5IrF_6 also at 285 K) with a Gemini A diffractometer equipped with an Atlas CCD detector using graphite monochromated MoKα radiation. The data were processed using the CrysAlisPro software suite program package [71]. Analytical absorption corrections were applied to all data sets. All structures were solved using the dual-space algorithm of the program SHELXT [72] implemented in the Olex crystallographic software [73]. Structure refinement for all structures was performed using the software SHELXL-2014 [74]. The crystals of the $Ni(XeF_2)_2(IrF_6)_2$ salt showed reproducible pseudo-merohedral twinning. This problem was solved at the data processing stage, and final refinement was performed using reflections from the main domain. The figures were created using the software Balls and Sticks [75]. The compound $XeF_5Nb_2F_{11}$ crystallizes in the acentric space group $P2_1$.

The very-close-to-zero value of the Flack's parameter (−0.031 (11)) confirms the correctness of the absolute structure.

The supplementary crystallographic data for this work are provided free of charge by the joint Cambridge Crystallographic Data Centre and the Fachinformationszentrum Karlsruhe Access Structures service www.ccdc.cam.ac.uk/structures (accessed on 10 March 2023): CSD-2246135 [$(Xe_2F_{11})_2NiF_6$], CSD-2246136 [$Ni(XeF_2)_2(IrF_6)_2$], CSD-2246137 [XeF_5AuF_6], CSD-2246138 [XeF_5IrF_6, 150 K], CSD-2246139 [$XeF_5Nb_2F_{11}$], CSD-2246140 [XeF_5PtF_6], CSD-2246141 [XeF_5RuF_6], CSD-2246142 [XeF_5IrF_6, 280 K], CSD-2246143 [$XeF_5Ta_2F_{11}$], CSD-2246144 [XeF_5NbF_6], CSD-2246145 [$XeF_5Ni(AsF_6)_3$], CSD-2246146 [XeF_5TaF_6], CSD-2246147 [XeF_5RhF_6].

5. Conclusions

Although the experiments to prepare $XeF_5M(BF_4)_x(SbF_6)_{3-x}$ (x = 1, 2, 3; M = Co, Mn, Ni, Zn), $XeF_5M(SbF_6)_3$ (M = Sn, Pb), and $XeF_5M(AF_6)_3$ salts (M = Cu, Ni; A = Cr, Nb, Ta, Ru, Rh, Re, Os, Ir, Pt, Au, As) were successful only in the preparation of $XeF_5Ni(AsF_6)_3$, further valuable results were obtained:

(a) In view of the successful preparation of $XeF_5Ni(AsF_6)_3$, we assume that it is reasonable to attempt the preparation of other compounds with other M^{2+} cations (M = Mg, Fe, Co, Zn, etc.).

(b) Crystal structure determination of XeF_5RhF_6 reveals a new type of structure. Together with the crystal structures of XeF_5TaF_6 and XeF_5IrF_6, which were determined for the first time, and the redetermined crystal structures of XeF_5NbF_6, XeF_5PtF_6, XeF_5RuF_6, and XeF_5AuF_6, they contribute to the understanding of the possible crystal phases in the family of XeF_5AF_5 salts.

(c) The crystal structures of the $XeF_5Nb_2F_{11}$ and $XeF_5Ta_2F_{11}$ salts were determined. These compounds were previously unknown, and for the $XeF_5A_2F_{11}$ salts, only the crystal structure of $XeF_5Sb_2F_{11}$ [25] was known. These three $[A_2F_{11}]^-$ salts are not isotypic and each of them represents a unique structural type.

(d) The crystal structure of XeF_5IrF_6 determined at 150 K and at room temperature is identical. The crystal structures of the salts XeF_5NbF_6, XeF_5PtF_6, XeF_5RuF_6, XeF_5AuF_6, XeF_5AsF_6 [37], and $(Xe_2F_{11})_2NiF_6$ redetermined at 150 K are also identical to those determined at room temperature, indicating that there is no phase transition in the range from 150 K to 298 K.

(e) All the new data on the XeF_5AF_6 and $XeF_5A_2F_{11}$ salts help to fill the gaps in our knowledge of the XeF_6-A^VF_5 system (Table 10).

(f) The preparation of $Ni(XeF_2)_2(IrF_6)_2$ has shown that it is worthwhile to try the preparation of some other $[M^{n+}(XeF_2)_p](AF_6)_n^-$ salts (A = Rh, Ru, Os, Ir, Pt, Au, Nb, Ta) where attempts to stabilize such salts with $[AF_6]^-$ (A = As, Sb) have failed.

Table 10. List of known xenon(VI) fluoridometallates including the determined crystal structures (letters in bold). Crystal structures reported in this work are highlighted in green.

Formula		**A^{5+}**											
$[Xe_2F_{11}][AF_6]$	**V** [a]	Nb [b]	Ta [c]	Ru [d]		Ir [e]	Pt [f]	**Au** [d]	U [g]	P [h]	As [i]	**Sb** [j]	Bi [k]
$[XeF_5][AF_6]$	V [l]	**Nb** [m]	**Ta** [c]	**Ru** [n]	**Rh** Os [o]	**Ir** [e]	**Pt** [p]	**Au** [f]	U [r]		**As** [s]	**Sb** [t]	Bi [u]
$[XeF_5][A_2F_{11}]$	V [l]	**Nb**	**Ta**									**Sb** [t]	

[a] Refs. [21,27], [b] Ref. [62], [c] Ref. [63], [d] Refs. [26,39], [e] Refs. [23,39], [f] Ref. [39], [g] Ref. [76], [h] Ref. [22], [i] Refs. [22,29], [j] Refs. [19,28], [k] Ref. [77], [l] Ref. [78], [m] Refs. [30,62], [n] Ref. [38], [o] Ref. [39], [p] Ref. [24], [r] Ref. [79], [s] Refs. [20,22,41], [t] Refs. [19,25], [u] Ref. [80].

Supplementary Materials: The following supporting information can be downloaded at: https://www.mdpi.com/article/10.3390/molecules28083370/s1, Table S1: Experimental conditions and observed products upon crystallization for the reactions between UV-irradiated F_2, XeF_2, MF_2 (M = Cu, Ni) and metal A (A = Ru, Rh, Re, Os, Ir, Pt), MF_3 (A = Cr, Au), and AF_5 (M = Nb, Ta, As), respectively, in anhydrous HF. The products observed upon crystallization and the experimental

conditions for the reactions between XeF_5SbF_6 and $M(SbF_6)_2$ (M = Sn, Pb) are also given.; Table S2: Experimental conditions and observed products upon crystallization in the experiments to prepare $XeF_5M(BF_4)_x(SbF_6)_{3-x}$ (x = 1, 2, 3; M = Co, Mn, Ni, Zn) salts.; Figures S1–S10. Raman spectra of XeF_5NbF_6, XeF_5TaF_6, XeF_5RhF_6, XeF_5RuF_6, XeF_5IrF_6, XeF_5PtF_6, $XeF_5Nb_2F_{11}$, $XeF_5Ta_2F_{11}$, O_2PtF_6, and O_2RuF_6 recorded on a single crystal; Figure S11. Raman spectra of single crystals after crystallization of the reaction product between XeF_2, Os powder and UV-irradiated F_2 in anhydrous HF: XeF_4 and unknown product.

Author Contributions: Conceptualization, Z.M.; formal analysis, Z.M. and E.G.; investigation, Z.M. and E.G.; writing—original draft preparation; visualization, Z.M. All authors have read and agreed to the published version of the manuscript.

Funding: The authors gratefully acknowledge financial support of the Slovenian Research Agency (research core funding No. P1–0045; Inorganic Chemistry and Technology).

Institutional Review Board Statement: Not applicable.

Informed Consent Statement: Not applicable.

Data Availability Statement: Not applicable.

Conflicts of Interest: The authors declare no conflict of interest.

Sample Availability: Samples of the compounds are available from the authors.

References

1. Slivnik, J.; Brčić, B.; Volavšek, B.; Marsel, J.; Vrščaj, V.; Šmalc, A.; Frlec, B.; Zemljič, Z. Über die syntheses von XeF_6. *Croat. Chem. Acta* **1962**, *34*, 253.
2. Slivnik, J.; Šmalc, A.; Žemva, B.; Mosevič, A.N. On the synthesis of xenon di-, tetra-, and hexafluoride. *Croat. Chem. Acta* **1968**, *40*, 49–51.
3. Chernick, C.L.; Malm, J.G. Xenon hexafluoride. In *Inorganic Synthesis*; Holtzclaw, F., Jr., Ed.; McGraw-Hill Book Company, Inc.: New York, NY, USA, 1966; Volume 8, pp. 258–260.
4. Žemva, B.; Slivnik, J. On the xenon-fluorine-reactions. *J. Inorg. Nucl. Chem. Suppl.* **1976**, *28*, 173–178. [CrossRef]
5. Nielsen, J.B.; Kinkead, S.A.; Purson, J.D.; Eller, P.G. New syntheses of xenon hexafluoride (XeF_6) and xenon tetrafluoride, (XeF_4). *Inorg. Chem.* **1999**, *29*, 1779–1780. [CrossRef]
6. Bartlett, N.; Sladky, F.O. The Chemistry of Krypton, Xenon and Radon. In *The Chemistry of the Monoatomic Gases, Comprehensive Inorganic Chemistry*; Bailar, J.C., Jr., Emeléus, H.J., Nyholm, R., Trotman-Dickenson, A.F., Eds.; Pergamon Press Ltd.: Oxford, UK, 1975; pp. 213–330.
7. Hoyer, S.; Emmler, T.; Seppelt, K. The structure of xenon hexafluoride in the solid state. *J. Fluor. Chem.* **2006**, *127*, 1415–1422. [CrossRef]
8. Schrobilgen, G.J.; Holloway, J.H.; Granger, P.; Brevard, C. Xenon-129 pulse Fourier-transfrom nuclear magnetic resonance spectroscopy. *Inorg. Chem.* **1978**, *17*, 980–987. [CrossRef]
9. Gavin, R.M., Jr.; Bartell, L.S. Molecular structure of XeF_6. I. Analysis of electron-diffrcation intensities. *J. Chem. Phys.* **1968**, *48*, 2460–2465. [CrossRef]
10. Bartell, L.S.; Gavin, R.M., Jr. Molecular structure of XeF_6. II. Internal motion and mean geometry deduced by electron diffraction. *J. Chem. Phys.* **1968**, *48*, 2466–2483. [CrossRef]
11. Gerken, M.; Hazendonk, P.; Nieboer, J.; Schrobilhen, G.J. NMR spectroscopic study of xenon fluorides in the gas phase and of XeF_2 in the solid state. *J. Fluor. Chem.* **2004**, *125*, 1163–1168. [CrossRef]
12. Dixon, D.A.; de Jong, W.A.; Peterson, K.A.; Christe, K.O.; Schrobilgen, G.J. Heats of formation of xenon fluorides and the fluoxionality of XeF_6 from high level electronic structure calculations. *J. Am. Chem. Soc.* **2005**, *127*, 8627–8634. [CrossRef]
13. Cheng, L.; Gauss, J.; Stanton, J.F. Relativistic coupled-cluster calculations on XeF_6: Delicate interplay between electron-correlation and basis-set effects. *J. Chem. Phys.* **2015**, *142*, 224309. [CrossRef]
14. Kaupp, M.; van Wüllen, C.; Franke, R.; Schmitz, F.; Kutzelnigg, W. The structure of XeF_6 and of compounds isoelectronic with it. A challenge to computational chemistry and to the qualitative theory of the chemical bond. *J. Am. Chem. Soc.* **1996**, *118*, 11939–11950. [CrossRef]
15. Gawrilow, M.; Becker, H.; Riedel, S.; Cheng, L. Matrix-isolation and quantum-chemical analysis of the C_{3v} conformer of XeF_6, $XeOF_4$, and their acetonitrile adducts. *J. Phys Chem. A* **2018**, *122*, 119–129. [CrossRef]
16. Sedgi, I.; Kozuch, S. Heavy atom tunnelling on XeF_6 pseudorotation. *Phys. Chem. Chem. Phys.* **2020**, *22*, 17725–17730. [CrossRef]
17. Paschoal, D.F.S.; Dos Santos, H.F. Predicting the structure and NMR coupling constant $^1J(^{129}Xe\text{-}^{19}F)$ of XeF_6 using quantum mechanics methods. *Phys. Chem. Chem. Phys.* **2021**, *23*, 7240–7246. [CrossRef]

18. Seppelt, K. Molecular hexafluorides. *Chem. Rev.* **2015**, *115*, 1296–1306. [CrossRef]
19. Gard, G.L.; Cady, G.H. Reactions of xenon hexafluoride with antimony pentafluoride, hydrogen chloride, and perfluorocyclopentane. *Inorg. Chem.* **1964**, *3*, 1745–1747. [CrossRef]
20. Selig, H. Xenon hexafluoride complexes. *Sciece* **1964**, *144*, 537.
21. Moody, G.J.; Selig, H. Vanadium pentafluoride complexes with xenon fluorides. *J. Inorg. Nucl. Chem.* **1966**, *28*, 2429–2430. [CrossRef]
22. Pullen, K.E.; Cady, G.H. The systems xenon hexafluoride-arsenic pentafluoride and xenon hexafluoride-phosphorus pentafluoride. *Inorg. Chem.* **1967**, *6*, 2267–2268. [CrossRef]
23. Bartlett, N.; Sladky, F.O. The relative fluoride ion donor abilities of XeF_2, XeF_4, and XeF_6 and a chemical purification of XeF_4. *J. Am. Chem. Soc.* **1968**, *90*, 5316–5317. [CrossRef]
24. Bartlett, N.; Einstein, F.; Stewart, D.F.; Trotter, J. The crystal structure of $[XeF_5]^+[PtF_6]^-$. *J. Chem Soc. A* **1967**, 1190–1193. [CrossRef]
25. Mazej, Z.; Goreshnik, E. Single-crystal structure determination of NO_2SbF_6, XeF_5SbF_6 and $XeF_5Sb_2F_{11}$. *J. Fluor. Chem.* **2015**, *175*, 47–50. [CrossRef]
26. Leary, K.; Zalkin, A.; Bartlett, N. Crystal structure of $Xe_2F_{11}{}^+AuF_6{}^-$ and the Raman spectrum of $Xe_2F_{11}{}^+$. *Inorg. Chem.* **1974**, *13*, 775–779. [CrossRef]
27. Benkič, P.; Golič, L.; Koller, J. Žemva, B. Crystal structure of $(Xe_2F_{11}{}^+)(VF_6{}^-)$. *Acta Chim. Slov.* **1999**, *46*, 239–252.
28. Mazej, Z.; Goreshnik, E. Crystal growth and characterization of the mixed-cation $Rb^+/[XeF_5]^+$ and $Cs^+/[XeF_5]^+$ salts. *Eur. J. Inorg. Chem.* **2017**, *2017*, 2800–2807. [CrossRef]
29. Bartlett, N.; Wechsberg, M. The xenon difluoride complexes $XeF_2{\cdot}XeOF_4$; $XeF_2{\cdot}XeF_6{\cdot}AsF_5$ and $XeF_2{\cdot}2XeF_6{\cdot}2AsF_5$ and their relevance to bond polarity and fluoride ion donor ability of XeF_2 and XeF_6. *Z. Anorg. Allg. Chem.* **1971**, *285*, 5–17. [CrossRef]
30. Žemva, B.; Golič, L.; Slivnik, J. Concerning xenon difluoride interactions with $XeF_5{}^+MF_6$, the existence of $XeF_2{\cdot}XeF_5{}^+RuF_6{}^-$ and the absence of $XeF_2{\cdot}XeF_5{}^+NbF_6{}^-$. *Vestn. Slov. Kem. Drus.* **1983**, *30*, 365–376.
31. Žemva, B.; Jesih, A.; Tepleten, D.H.; Zalkin, A.; Chhetman, A.K.; Bartlett, N. Phases in the system XeF_2/XeF_5AsF_6 and structural and vibrational evidence for the following ionization pathway: XeF_2 $XeF^+ + F^-$. *J. Am. Chem. Soc.* **1987**, *109*, 7420–7427. [CrossRef]
32. Lozinšek, M.; Mercier, H.P.A.; Schrobilgen, G.J. Mixed noble-gas compounds of krypton(II) and xenon(VI): $[F_5Xe(FKrF)AsF_6]$ and $[F_5Xe(FKrF)_2AsF_6]$. *Angew. Chem. Int. Ed.* **2021**, *60*, 8149–8156. [CrossRef]
33. Pointner, B.E.; Suotamo, R.J.; Schrobilgen, G.J. Syntheses and X-ray crystal structures of α- and β-$[XeO_2F][SbF_6]$, $[XeO_2F][AsF_6]$, $[FO_2XeFXeXeO_2F][AsF_6]$, and $[XeF_5][SbF_6]{\cdot}XeOF_4$ and computational studies of the XeO_2F^+ and $FO_2XeFXeO_2F^+$ cations and related species. *Inorg. Chem.* **2006**, *45*, 1517–1534. [CrossRef]
34. Mazej, Z.; Goreshnik, E. $[XeF_5]^+$/metal and $[XeF_5]^+$/non-metal mixed-cation salts of hexafluoridoantimonate(V). *Eur. J. Inorg. Chem.* **2015**, *8*, 1453–1456. [CrossRef]
35. Mazej, Z.; Goreshnik, E. Influence of the increasing size of the M^{2+} cation on the crystal structures of $XeF_5M(SbF_6)_3$ (M = Ni, Mg, Cu, Zn, Co, Mn, Pd) and $(XeF_5)_3[Hg(HF)]_2(SbF_6)_7$. *Eur. J. Inorg. Chem.* **2016**, *2016*, 3156–3364. [CrossRef]
36. Mazej, Z.; Goreshnik, E. Mixed cation $[H_3O]^+/[XeF_5]^+/M^{2+}$ (M = Ca, Cd), $[O_2]^+/[XeF_5]^+/Sr^{2+}$ and $[H_3O]^+/Sr^{2+}$ fluoridoantimonate(V) salts. *Z. Anorg. Allg. Chem.* **2022**, *648*, e202200173.
37. Goreshnik, E.; Akselrud, L.G.; Mazej, Z. Mixed-anion $[AsF_6]^-/[SbF_6]^-$ salts of Cs^+ and $[XeF_5]^+$; incommensurately modulated crystal structures of $[XeF_5][As_{1-x}Sb_xF_6)$ (x ≈ 0.5 and 0.7). *Cryst. Growth Des.* **2022**, *22*, 2980–2988. [CrossRef]
38. Bartlett, N.; Gennis, M.; Gibler, D.D.; Morrell, B.K.; Zalkin, A. Crystal structures of $[XeF^+][RuF_6{}^-]$ and $[XeF_5{}^+][RuF_6{}^-]$. *Inorg. Chem.* **1973**, *12*, 1717–1721. [CrossRef]
39. Bartlett, N.; Leary, K. Quinquevalent gold salts. *Rev. Chim. Minér.* **1976**, *13*, 82–97.
40. Jesih, A.; Lutar, K.; Leban, I.; Žemva, B. Synthesis and crystal structure of $(Xe_2F_{11}{}^+)_2NiF_6{}^{2-}$. *Inorg. Chem.* **1989**, *28*, 2911–2914. [CrossRef]
41. Bartlett, N.; DeBoer, B.G.; Hollander, F.J.; Sladky, F.O.; Templeton, D.H.; Zalkin, A. Crystal structures of $[Xe_2F_3{}^+][AsF_6{}^-]$ and $[XeF_5{}^+][AsF_6{}^-]$. *Inorg. Chem.* **1974**, *13*, 780–785. [CrossRef]
42. Mazej, Z.; Arčon, I.; Benkič, P.; Kodre, A.; Tressaud, A. Compressed octahedral coordination in chain compounds containing divalent copper: Structure and magnetic properties of $CuFAsF_6$ and $CsCuAlF_6$. *Chem. Eur. J.* **2004**, *10*, 5052–5058. [CrossRef]
43. Botkovitz, P.; Lucier, G.M.; Rao, R.P.; Bartlett, N. The crystal structure of $O_2{}^+RuF_6{}^-$ and the nature of O_2RhF_6. *Acta Chim. Slov.* **1999**, *46*, 141–154.
44. Ibers, J.A.; Hamilton, W.C. Crystal structure of O_2PtF_6: A neutron-diffraction study. *J. Chem. Phys.* **1966**, *44*, 1748–1752. [CrossRef]
45. Mazej, Z.; Goreshnik, E. Crystal growth and crystal structures of gold(V) compounds: $Cu(AuF_6)_2$, $Ag(AuF_6)_2$, and $O_2(CuF)_3(AuF_6)_4{\cdot}HF$. *Eur. J. Inorg. Chem.* 2023, in press. [CrossRef]
46. Mazej, Z. Fluoride ion donor ability of binary fluorides towards the Lewis acids AsF_5 and SbF_5. *J. Fluor. Chem.* **2023**, *265*, 110073. [CrossRef]
47. Mazej, Z. Photochemical Syntheses of Fluoride. In *Modern Synthesis Processes and Reactivity of Fluorinated Compounds*; Groult, H., Leroux, F., Tressaud, A., Eds.; Elsevier Inc.: London, UK, 2017; pp. 587–607.
48. Whalen, J.M.; Lucier, G.M.; Bartlett, N. The room temperaure conversion of nickel difluoride to hexafluoronickelate(IV) salts of alkali cations. *J. Fluor. Chem.* **1998**, *88*, 107–110. [CrossRef]

49. Higelin, A.; Riedel, S. High Oxidation States in Transition Metal Fluorides. In *Modern Synthesis Processes and Reactivity of Fluorinated Compounds*; Groult, H., Leroux, F., Tressaud, A., Eds.; Elsevier: London, UK, 2017; pp. 561–586.
50. Lutar, K.; Leban, I.; Ogrin, T.; Žemva, B. $XeF_2 \cdot CrF_4$ and $(XeF_5^+CrF_5^-)_4 \cdot XeF_4$; syntheses, crystal structures and some properties. *Eur. J. Solid State Inorg. Chem.* **1992**, *29*, 713–727.
51. Mazej, Z.; Goreshnik, E. Alkali metal (Li^+–Cs^+) salts with hexafluorochromate(V), hexafluorochromate(IV), pentafluorochromate(IV), and undecafluorodichromate(IV) anions. *Eur. J. Inorg. Chem.* **2008**, *2008*, 1795–1812. [CrossRef]
52. Lutar, K.; Borrmann, H.; Žemva, B. $XeF_2 \cdot 2CrF_4$ and $XeF_5^+CrF_5^-$: Syntheses, crystal structures, and some properties. *Inorg. Chem.* **1998**, *37*, 3002–3006. [CrossRef]
53. Bortolus, M.R.; Mercier, H.P.A.; Nguyen, B.; Schrobilgen, G.J. Syntheses and characterizations of the mixed noble-gas compounds, $[FKr^{II}FXe^{II}F][AsF_6] \cdot 0.5Kr^{II}F_2 \cdot 2HF$, $([Kr^{II}{}_2F_3][AsF_6])_2 \cdot Xe^{IV}F_4$, and $Xe^{IV}F_4 \cdot Kr^{II}F_2$. *Angew. Chem. Int. Ed.* **2021**, *60*, 23678–23686. [CrossRef]
54. Mazej, Z.; Goreshnik, E. Synthesis, Raman spectra and crystal structures of $[Cu(XeF_2)_n](SbF_6)_2$ (n = 2, 4). *Inorg. Chem.* **2008**, *47*, 4209–4214. [CrossRef]
55. Bondi, A. van der Waals volumes and radii. *J. Phys. Chem.* **1964**, *68*, 441–451. [CrossRef]
56. Shannon, R.D. Revised effective ionic radii and systematic studies of interatomic distances in halides and chaleogenides. *Acta Crystallogr. Sect. A* **1976**, *32*, 751–767. [CrossRef]
57. Graudejus, O.; Wilkinson, A.P.; Chacón, L.C.; Bartlett, N. M-F interatomic distances and effective volumes of second and third transition series MF_6^- and MF_6^{2-} anions. *Inorg. Chem.* **2000**, *39*, 2794–2800. [CrossRef]
58. Röhr, C.; Kniep, R. Die kristalstrukturen von $Li[PF_6]$ und $Li[AsF_6]$: Zur kristalchemie von verbindungen $A[E^VF_6]$. *Z. Naturforsch.* **1994**, *49b*, 650–654. [CrossRef]
59. Burns, J. The crystal structure of lithium fluoroantimonate(V). *Acta Cryst.* **1962**, *15*, 1098–1101. [CrossRef]
60. Mazej, Z.; Hagiwara, R. Hexafluoro-, heptafluoro-, and octafluoro-salts, and $[M_nF_{5n+1}]^-$ (n = 2, 3, 4) polyfluorometallates of singly charged metal cations, Li^+–Cs^+, Cu^+, Ag^+, In^+ and Tl^+. *J. Fluor. Chem.* **2007**, *128*, 423–437. [CrossRef]
61. Mazej, Z.; Goreshnik, E. Photochemical preparation of $CsMF_6$ salts (M = Ru, Rh, Os, Ir, Pt); crystal structures and Raman spectra. *J. Fluor. Chem.* 2023, in press. [CrossRef]
62. Žemva, B.; Slivnik, J. On the syntheses of xenon(VI) fluoroniobates(V). *J. Fluor. Chem.* **1976**, *8*, 369–371. [CrossRef]
63. Aubert, J.; Cady, G.H. The systems xenon hexafluoride–tantalum pentafluoride, xenon hexafluoride–manganese fluoride, xenon hexafluoride–uranium pentafluoride. *Inorg. Chem.* **1970**, *9*, 2600–2602.
64. Marchetti, F.; Pampaloni, G.; Pinzino, C.; Zacchini, S. Stable $[M_2F_{11}]^-$ (M = Nb, Ta) salts of protonated 1,3-dimethoxybenzene. *Eur. J. Inorg. Chem.* **2013**, *2013*, 5755–5761. [CrossRef]
65. Tramšek, M.; Žemva, B. Synthesis, properties and chemistry of xenon(II) fluoride. *Acta Chim. Slov.* **2006**, *53*, 105–116. [CrossRef]
66. Mazej, Z.; Goreshnik, E. Crystal growth from anhydrous HF solutions of M^{2+} (M = Ca, Sr,. Ba) and $[AuF_6]^-$, not only simple $M(AuF_6)_2$ salts. *Inorg. Chem.* **2022**, *61*, 10587–10597. [CrossRef] [PubMed]
67. Šmalc, A.; Lutar, K. Xenon difluoride (modification). In *Inorganic Syntheses*; Grimes, R.N., Ed.; John Wiley & Sons, Inc.: New York, NY, USA, 1992; Volume 29, pp. 1–4.
68. Mazej, Z. Žemva, Synthesis of arsenic pentafluoride by static fluorination of As_2O_3 in a closed system. *J. Fluor. Chem.* **2005**, *126*, 1432–1434. [CrossRef]
69. Mazej. Z. Recent achievements in the synthesis and characterization of metal hexafluorantimonates and hexafluoroaurates. *J. Fluor. Chem.* **2004**, *125*, 1723–1733. [CrossRef]
70. Gantar, D.; Leban, I.; Frlec, B.; Holloway, J.H. Metal(II) hexafluoroantimonates: Preparation and characterization of $MF_2 \cdot 2SbF_5$ (M = Mg, Ni, Zn, Fe, Co, Cu, Cr, Ag, Cd, or Pb) and the X-ray structure determination of $AgF_2 \cdot 2SbF_5$. *J. Chem. Soc. Dalton Trans.* **1987**, *10*, 2379–2383. [CrossRef]
71. *CrysAlisPro*; Version 1.171.37.31. release 14 January 2014 CrysAlis171.NET; Agilent Technologies: Santa Clara, CA, USA, 2014.
72. Sheldrick, G.M. SHELXT-Integrated space-group and crystal-structure determination. *Acta Crystallogr. Sect. A* **2015**, *71*, 3–8. [CrossRef]
73. Dolomanov, O.V.; Bourhis, L.J.; Gildea, R.J.; Howard, J.A.K.; Puschmann, H. OLEX2: A complete structure solution, refinement and analysis program. *J. Appl. Crystallogr.* **2009**, *42*, 339–341. [CrossRef]
74. Sheldrick, G.M. Crystal structure refinement with SHELXL. *Acta Crystallogr. Sect. C* **2015**, *71*, 3–8. [CrossRef]
75. Ozawa, T.C.; Kang, S.J. Balls&Sticks: Easy-to-use structure visualization and animation program. *J. Appl. Crystallogr.* **2004**, *37*, 679.
76. Slivnik, J.; Frlec, B.; Žemva, B.; Bohinc, M. Xenon hexafluoride-uranium pentafluoride complexes. *J. Inorg. Nucl. Chem.* **1970**, *32*, 1397–1400. [CrossRef]
77. de Waard, H.; Bukspan, S.; Schrobilgen, G.J.; Holloway, J.H.; Martin, D. A Mössbauer study of xenon compounds. *J. Chem. Phys.* **1979**, *70*, 3247–3253. [CrossRef]
78. Jesih, A.; Žemva, B.; Slivnik, J. Reactions in the system vanadium pentafluoride–xenon hexafluoride. *J. Fluor. Chem.* **1982**, *19*, 231–236. [CrossRef]

79. Frlec, B.; Bohinc, M.; Charpin, P.; Drifford, M. On the xenon hexafluoride–uranium pentafluoride XeF_6UF_5. *J. Inorg. Nucl. Chem.* **1972**, *34*, 2938–2941. [CrossRef]
80. Družina, B.; Žemva, B. On the synthesis of xenon(VI) hexafluorobismutathe(V). *J. Fluor. Chem.* **1988**, *39*, 309–315. [CrossRef]